

Lehigh University

Lehigh Preserve

Theses and Dissertations

5-1-2018

Bubbles and Dust: Experimental Results of Dissolution Rates from Metal Salts and Glasses in Volcanic Ash Deposits

Candace Wygel

Lehigh University, candacewygel@gmail.com

Follow this and additional works at: <https://preserve.lehigh.edu/etd>

Recommended Citation

Wygel, Candace, "Bubbles and Dust: Experimental Results of Dissolution Rates from Metal Salts and Glasses in Volcanic Ash Deposits" (2018). *Theses and Dissertations*. 5719.
<https://preserve.lehigh.edu/etd/5719>

This Thesis is brought to you for free and open access by Lehigh Preserve. It has been accepted for inclusion in Theses and Dissertations by an authorized administrator of Lehigh Preserve. For more information, please contact preserve@lehigh.edu.

**Bubbles and Dust: Experimental Results of Dissolution Rates from Metal Salts and
Glasses in Volcanic Ash Deposits**

By

Candace M. Wygel

A Thesis

Presented to the Graduate and Research Committee

of Lehigh University

in Candidacy for the Degree of

Master of Science

in

Earth and Environmental Sciences

Lehigh University

May 2018

© 2018 Copyright

Candace Wygel

Thesis is accepted and approved in partial fulfillment of the requirements for the Master
of Science in Earth and Environmental Sciences

“Bubbles and Dust: Experimental Results of Dissolution Rates from Metal Salts and
Glasses in Volcanic Ash Deposits”

Candace M. Wygel

Date Approved

Dork L. Sahagian
(Advisor)

Stephen C. Peters
(Committee Member)

Jill McDermott
(Committee Member)

David J. Anastasio
(Department Chair)

Acknowledgements

The author would like to thank her advisor Dr. Dork Sahagian for supporting her and being an invaluable resource throughout her Master's program. She deeply appreciates his trust and unfailing confidence in her. She would also like to thank Dr. Stephen Peters and Dr. Jill McDermott for being exceptional mentors and for sharing their wisdom of geochemistry. She could not have asked for a more helpful and supportive committee to guide her throughout the Master's thesis; and the author wants to thank each of them from the bottom of her heart for helping her grow as a scientist.

The author would like to thank the Lehigh's Earth and Environmental Science Department and the College of Arts and Sciences for funding her research. Without this support, the research would have not been possible. She would like to thank Don Swanson, Gino González, and Joe Liccardi for collecting and providing her pristine volcanic ash samples. The author appreciates Dr. Kai Landskron and Dr. Mark Snyder for use of their labs and instruments, and especially to their graduate students Yiqun Liu and Megha Sharma for their instruction and guidance. Additionally, she would like to give a sincere thank you to George Yasko who always was willing to assist with experimental challenges and to offer a good joke.

Furthermore, she would like to thank the people that she met on her journey as a Master's student. She is very grateful to the members of her research group; Leslie Tintle and Megan Clark; Leslie for her thoughtful edits, being an incredible support and a true

friend, and Megan for her continued guidance throughout the years and being a great “big sister”. Thanks to my office-mate, Eli, for never failing to amuse me. Likewise, the author would like to thank the Lehigh University’s Earth and Environmental Science Department faculty, staff, and graduate students. To all her friends that she has made here at Lehigh, she is so grateful for their friendship, as her experience would have been entirely different without them. Lastly, she would like to thank her parents for their confidence and love, supporting her passion for geology, and being there for her every step of the way.

Table of Contents

Title Page.....	i
Copyright Page.....	ii
Approval Page.....	iii
Acknowledgements.....	iv
Table of Contents.....	vi
List of Tables.....	viii
List of Figures.....	ix
1. Abstract.....	1
2. Introduction.....	2
3. Scope and Implications	
3.1 Scientific Scope.....	3
3.2 Implications.....	4
4. Background	
4.1 Chemical Impacts of Ash Leachates.....	5
4.2 Volcanic Ash Surface Area.....	9
4.3 Geologic Setting.....	13
5. Hypotheses.....	15
6. Methods	
6.1 Ash samples.....	17
6.2 Surface Area Analysis.....	20
6.3 Ash Leachate Experimentation: CLT.....	23
6.4 Geochemical Analyses.....	25

7. Results	
7.1 Surface Area.....	26
7.2 Chemistry.....	32
7.3 Pele's Spheres.....	43
7.4 Experimental Uncertainties.....	45
8. Discussion	
8.1 Trends in BET and Geometric Surface Areas.....	46
8.2 Metal Salts and Glass Dissolution	50
8.3 Environmental Implications.....	51
9. Conclusions.....	53
10. Future Research.....	54
11. References.....	56
12. Appendices.....	65
13. Vita.....	69

List of Tables

Table 1. A summary of adverse human health impacts from volcanic ash water contamination from Stewart et al., 2006. Concentrations are reported in mg/L.....	7
Appendix A. Fluxes of Al and Si from the Jones and Gislason (2008) leaching experiment of volcanic ash in de-ionized water. Flux results from this study are overlaid on the figure.....	65
Appendix B. Measured particle size distribution, using the SEM and Image J, of Eyjafjallajökull (left column) and Kilauea (right column) ash over one week. Frequency of particles is plotted on the Y-axis and binned sizes of the particles in μm is on the X-axis. Subscripts equal the time that the ashes were leached for. 0: Initial ash before leachate test, 1: Post 1 hour of leaching, 2: Post 8 hours of leaching, 3: Post 4 days of leaching, 4: Post 7 days of leaching. Greatest number density of particles is $< 20 \mu\text{m}$ for both populations.....	66
Appendix C. SEM images of the gypsum Turrialba precipitated weeks after the leaching experiment. Gypsum chemistry was confirmed using EDS.....	67
Appendix D. Chemical concentrations from ICP-MS and IC. BET and geometric surface area data. Mass, pH, and flow rate data. Calculated flux data and dissolution rates calculated with both BET and geometric surface areas: Attached as supplemental data files	68
Appendix E. Column leachate test data from Redoubt, Turrialba, Eyjafjallajökull, and Kilauea: Attached as supplemental data files	68

List of Figures

- Figure 1.** A schematic diagram demonstrating the release of ash and gas into the atmosphere, and the chemical interactions between them. Acid magmatic gasses (HF, HCl, SO₂) are erupted along with ash, water vapor and CO₂. These gasses adsorb onto the ash surfaces and create metal salts. Ash is aggregated and begins to fall out of the ash cloud. The ash is eventually deposited, interacts with water, and is leached into the environment (adapted from USGS, 2010)..... 6
- Figure 2.** Fluoride concentration over 0-300 days in the Ytri-Rangá River after the 1991 eruption of Mt. Hekla, Iceland. Dashed horizontal lines represent the upper limit for safe drinking water (Flaathen and Gislason, 2007)..... 8
- Figure 3.** SEM images of the four pristine, unhydrated ash samples prior to leaching. Left column of images shows a larger population view while the right column shows one representative particle from each eruption: A) Redoubt ash, B) Turrialba ash, C) Eyjafjallajökull ash, and D) Kilauea ash..... 18
- Figure 4.** Column Leachate Tests (CLT) for week-long experiments. Milli-Q source water is pumped through four Teflon tubes at a constant flow rate using a peri pump. The water travels up through four identical columns packed with ash sitting vertically in a thermostatic water bath. The water then goes out to collection for analysis or to waste.. 24
- Figure 5.** Geometric and BET surface area data for all ash samples throughout the leaching experiment, measured in m²/g. Geometric surface area is plotted on the primary (left) Y-axis and BET surface area is plotted on the secondary (right) Y-axis, and time of

the leaching experiment is on the X-axis. The observed trends represent the disaggregation, dissolution, and weathering of the ash particles..... 27

Figure 6. BET surface areas for all ash samples over one week measured in m^2/g . Time is plotted in days. Andesitic ashes (Turrialba & Redoubt) show an initial increasing trend in surface area then gradual decrease, representing disaggregation and dissolution of the ash whereas basaltic ashes (Eyjafjallajökull & Kilauea) show an initial decrease and then gradual increase in surface area, representing dissolution and then weathering of the ash particles..... 27

Figure 7. Measured particle size distribution, using the SEM and Image J, of Turrialba (left column) and Redoubt (right column) ash over one week. Frequency of particles is plotted on the Y-axis and binned sizes of the particles in μm is on the X-axis. Subscripts equal the time that the ashes were leached for. 0: Initial ash before leachate test, 1: Post 1 hour of leaching, 2: Post 8 hours of leaching, 3: Post 4 days of leaching, 4: Post 7 days of leaching. Greatest number density of particles is $< 20 \mu\text{m}$ for both populations..... 29

Figure 8. Calculated geometric surface areas for all ash samples over one week measured in m^2/g . Time is plotted in days. Geometric surface area only incorporates particles $> 5 \mu\text{m}$. All ashes show an initial increasing trend in surface area then gradual decrease over the remainder of the leaching experiment. This trend represents the disaggregation and dissolution of the ashes..... 30

Figure 9. SEM images of Turrialba ash throughout the leaching experiment at four different time intervals; initially, post 8 hours, post 4 days, and post 7 days. This time

series demonstrates the balding effect which consists of the disaggregation and dissolution of the dust particles into the leachate.....	31
Figure 10. SEM image of a Pele’s sphere after it had been leached for 1 hour. This image demonstrates the mud-crack weathering pattern, unique to these spherules. While this pattern was commonly seen in the ash after leaching, it was only observed on a small population of particles after the entire week of leaching.....	33
Figure 11. Ternary diagram from Witham et al. (2005) showing the relative SO_4^{2-} , Cl, and F (x10) absorbed mass concentrations from a compilation of ash leachate analyses, including the current study. Points from this ash leachate analysis represent the chemistry after the initial 30 minutes of leaching. Light blue and light green dots represent the chemistry of the leachate after an hour for Turrialba and Kilauea respectively.....	34
Figure 12. Concentrations ($\mu\text{mol/kg}$), flow rates (mL/min), and dissolution rates ($\text{mol/m}^2\text{s}$) of major elements from all volcanic ash samples against time (days) over the week-long experiment. A) Redoubt, B) Turrialba, C) Eyjafjallajökull, and D) Kilauea. Rapid initial decay in concentration and dissolution rate seen in all samples. Two chemical populations seen in Kilauea and potentially in Turrialba.....	38
Figure 13. pH of volcanic ash leachates for all samples over the week-long leaching experiment plotted against time in days. There is an initial decrease in all samples and then a gradual increase towards a neutral pH towards the end of the week. This provides evidence for the dissolution of the acid magmatic gasses which initially dissociate to lower pH.....	39

Figure 14. Accumulated concentrations ($\mu\text{mol/kg}$) of health-relevant elements (As, Cd, Cr, Cu, F, and Se) after 1-hour of leaching. The solid black line represents the WHO upper limit for safe drinking water standards. Kilauea, the chemical (basaltic) endmember, and Turrialba, the surface area endmember, consistently leach the highest concentrations..... 42

Figure 15. Accumulated fluoride concentrations ($\mu\text{mol/kg}$) over the first day of the leaching experiment for all ash samples. The WHO dashed-line marks the upper limit for safe drinking water. Kilauea, the chemical (basaltic) endmember, and Turrialba, the surface area endmember, leach the highest concentration of fluoride..... 43

Figure 16. SEM (upper) and optical microscope images (lower) of the interior of a few Pele's spherules. The above SEM image correlates with lower optical microscope image below it. The images show the differences in the internal vesicle distribution. The images on the left show little to no vesicles, the middle images show some vesicles of varying sizes, and the right images show many vesicles with some directionality to them. The optical microscope is very helpful to analyze the interior of these spherules because it allows us to see through the translucent sphere..... 44

1. Abstract

Volcanic eruptions are natural hazards due to their explosive nature and widespread atmospheric transportation and deposition of ash particles. After deposition and subsequent leaching in soils or water bodies, volcanic ash can lead to chemically altered water, positively and negatively impacting the health of flora and fauna, including humans. This study determined the control of ash surface area and chemical composition on ash dissolution rates. Fresh, unhydrated ash samples from four volcanoes with diverse environments and morphology, from Pele's spheres to dusty vesicular ash, were analyzed in the laboratory. Column Leachate Tests (CLT) were used to compare leaching rates over a range of basaltic to andesitic ashes as a function of time and surface area, to recreate the effects of ash deposition. Ash morphology was characterized on the SEM before and during leaching in order to calculate geometric surface area. Specific surface area was quantified throughout the leaching experiment by multi-point Brunauer Emmett Teller (BET) analysis. It was found that surface area, measured both geometrically and by BET, generally increases for a short time, gradually decreases, then increases over the rest of the leaching experiment, due to area to mass ratio fluctuations. After the CLT, post-leaching water analyses for elemental compositions were conducted by ICP-MS and IC. Steady state dissolution rates initially decayed rapidly due to the smallest size fraction of ash (dust) which provides high surface area with a great amount of fresh leachable surfaces as well as the rapid dissolution of highly soluble metal salts. Some water concentrations of elements of concern to human and ecosystem health such as F, Cd, Se, As, Cr, were above WHO drinking water standards after the first hour after ash deposition completes, depending on bioaccumulation and chronic exposure, the water

may be safe for consumption. This has applications to emergency response and preparedness in volcanic regions.

2. Introduction

Volcanic eruptions are natural hazards due to their explosive nature and widespread transportation and deposition of ash particles. After deposition and subsequent leaching in soils or water bodies, volcanic ash can lead to chemically altered water, positively and negatively impacting the health of flora and fauna, including humans. Ash morphology and chemistry varies around the world depending on tectonic setting. Subduction zone or hot spot volcanoes located on oceanic crust often produce physically and chemically varying mafic ashes, and volcanoes on continental crust typically produce a range of silicic ashes. Both chemistry and morphology can vary widely and effect the rate of leaching anions and cations into the environment.

This study characterizes the geochemical effect of ash leachates, the liquid byproduct after ash encounters water, on the natural environment by determining the impact of ash morphology and chemistry on dissolution rates. By studying the water chemistry after contact with volcanic ash from various eruptions, potential hazards and benefits can be identified for specific volcanic ash compositions. This study aims to bring a better understanding of the controls on leaching rates and consequently how diverse ash leachates affect the environment over time.

3. Scope and Implications

3.1 *Scientific Scope*

This study provides a natural analog for the geochemical effects of ash leachates on the natural environment. Ash leachate studies have been completed both in the field and the laboratory (Frogner et al., 2001; Witham et al., 2005; Frogner Kockum et al., 2006; Flaathen and Gislason, 2007; Jones and Gislason 2008; Genareau et al., 2016; Bosshard-Stadlin et al., 2017; Cangemi et al., 2017), including studies of leachate chemistry from a range of compositions from andesitic to basaltic ash (Jones and Gislason, 2008). Similar leachate studies have used previously weathered ash (Jones and Gislason 2008; Genareau et al., 2016), while others use unhydrated pristine ash (Gislason et al., 2011, Olgun et al., 2011; Cronin et al., 2014) to understand various environmental geochemical conditions and processes, post volcanic eruptions. For this study, pristine ash is used and defined as natural ash, collected immediately after an eruption, that has not been altered naturally by precipitation (unhydrated) or mechanically in the lab. Pristine ash provides the opportunity to understand how natural ash morphology and volcanic dust affect surface area. There has yet to be a study which quantifies the effects of surface area (ash morphology) and chemistry on leaching rates over time. Previous studies have assumed a non-changing surface area (Wolff-Boenisch et al., 2004; Jones and Gislason 2008). In this study, ash surface area was measured throughout four distinct, week-long leaching experiments, which provided us with a greater understanding of how dissolution rates were impacted by changing surface area. Understanding surface area fluctuations in conjunction with leachates from pristine ash allows us to better understand how people and the ecosystem are impacted by chemically altered water during and throughout a

volcanic eruption. This has applications to emergency response and preparedness in volcanic regions.

3.2 Implications

Volcanic eruptions consistently affect the global ecosystem, and while some hazards are well known, geochemical impacts from ejecta are not as well understood. There are many geologic hazards caused by volcanoes such as tephra fall and ballistic projectiles, volcanic gas emissions, lava flows, earthquakes, tsunamis, landslides, lahars, and pyroclastic density currents (PDCs); all of which are common, well-known hazards. Other volcanic hazards affect technology such as aviation dangers (Albersheim and Guffanti, 2008) recently seen in 2010 when the Eyjafjallajökull eruption disrupted European air travel (Gislason et al., 2011). There are also a wide range of human health impacts associated with volcanic eruptions such as inhalation dangers, building collapse, and drinking water contamination (Baxter and Ancia, 2002; Horwell et al., 2003; <http://www.ivhhn.org/>). This study focused on the chemical impacts of ash leachates from volcanic ash with varying morphology and chemical composition, which provides insight into how surface water may be altered by interaction with freshly deposited volcanic ash. Volcanic ash leachates have both poisoning and fertilizing potential; by contaminating water, making it unsafe for human and animal consumption, and enriching volcanic soils with critical nutrients.

4. Background

4.1. *Chemical Impacts of Ash Leachates*

Volcanic ash, after deposition on soil or in water, leaches and subsequently leads to elevated anion and cation concentrations. Volcanic glass is highly soluble; rapidly mechanically and chemically weathering, which allows us to see immediate chemical changes in the environment after volcanic eruptions. Volcanic ash leachates are important to study because it allows us to understand the positive and negative chemical impacts that volcanic eruptions can have on the ecosystem. Volcanic aerosols in an ash plume consist of acid magmatic gases (HF, HCl, SO₂) that adsorb onto the surface of volcanic ash particles and form deliquescent metal salt encrustations (crust of highly soluble metal salts), such as fluorides, chlorides, and sulfates (Óskarsson, 1980; Óskarsson, 1981; Frogner et al., 2001; Cronin et al., 2014) (**Figure 1**). These encrusted surfaces are thus extremely water-soluble and dissolve rapidly to release ions into the resulting soil and surface water (Óskarsson, 1981; Frogner et al., 2001). Released nutrients and trace metals have both poisoning and fertilizing potential.

The elevated concentrations of dissolved ions leached from volcanic ash, such as Cl, F, Al, Fe, Mn, As, Cd, Cr, Cu, Pb, Se, and Zn, can alter the pH of the water and render it unsafe or undrinkable for human and animal consumption (Stewart et al., 2006; Flaathen and Gislason, 2007; Wilson et al., 2010; Genareau et al., 2016) (**Table 1**).

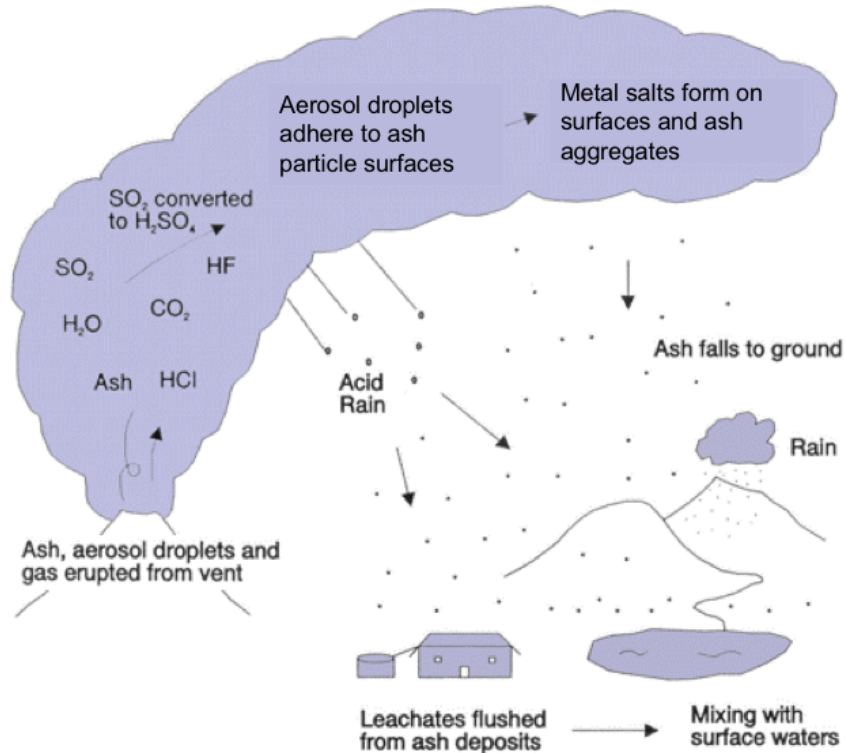


Figure 1. A schematic diagram demonstrating the release of ash and gas into the atmosphere, and the chemical interactions between them. Acid magmatic gasses (HF, HCl, SO₂) are erupted along with ash, water vapor and CO₂. These gasses adsorb onto the ash surfaces and create metal salts. Ash is aggregated and begins to fall out of the ash cloud. The ash is eventually deposited, interacts with water, and is leached into the environment (adapted from USGS, 2010).

Heavy metals are of particular concern when leached into the environment since they can bioaccumulate, may be toxic in low concentrations, and do not degrade. Although some ions (Mn, Fe, Na, SO₄²⁻, Zn) do not render water toxic, they still make it undrinkable for humans (Stewart et al., 2006). High levels of fluoride (F) have been frequently measured in volcanic ash leachates (Araya et al., 1990; Rubin et al., 1994; Cronin and Sharp, 2002; Cronin et al., 2003; Thordarson et al., 2003; Stewart et al., 2006; Flaathen and Gislason, 2007; Cordeiro et al., 2012; Madonia et al., 2013) (**Figure 2**).

Table 1. A summary of adverse human health impacts from volcanic ash water contamination from Stewart et al., 2006. Concentrations are reported in mg/L.

		USEPA ^a		WHO ^b	New Zealand ^c		Japan ^d	Potential effects if standard exceeded ^e
		Primary standards (MCLs)	Secondary standards	Health standards	Health MAVs	Aesthetic GVs		
<i>Elements of health significance</i>								
Antimony	Sb	0.006		0.02	0.02			Increase in blood cholesterol; decrease in blood sugar
Arsenic	As	0.01		0.01	0.01		0.01	Skin damage, increased cancer risk
Barium	Ba	2		0.7	0.7			Hypertension
Boron	B			0.5	1.4		1.0	May affect male reproductive tract
Bromate ^f	Br	0.01		0.01	0.01		0.01	Increased cancer risk
Cadmium	Cd	0.005		0.003	0.004		0.01	Kidney damage
Chromium	Cr	0.1		0.05	0.05		0.05	Allergic dermatitis
Copper	Cu	2		2	2		1	Liver or kidney damage
Fluoride	F	4		1.5	1.5		0.8	Dental and skeletal fluorosis
Lead	Pb	0.015		0.01	0.01		0.01	Impairs development and learning in children
Lithium	Li				1			g
Molybdenum	Mo			0.07	0.07			g
Mercury	Hg	0.002		0.001	0.002		0.0005	Kidney damage
Nickel	Ni			0.02	0.02			g
Nitrate	NO ₃	44.3		50	50		44.3	Can cause blue-baby syndrome in infants
Selenium	Se	0.05		0.01	0.01		0.01	Liver or kidney damage; damage to circulation and nervous systems
Thallium	Tl	0.002						Blood, kidney, liver or intestine problems
<i>Elements influencing drinking water acceptability</i>								
Acidity	H ⁺		pH 6.5–8.5		pH 7–8.5	pH 5.8–8.6		Low pH: bitter metallic taste, corrosion High pH: soapy feel, soda taste
Aluminium	Al		0.05–0.2		0.1	0.2		Floc deposits, discolouration
Chloride	Cl		250		250	200		Salty taste
Copper	Cu		1		1	1		Metallic taste, blue-green staining
Hardness	Ca				200	300		Scale deposits and scum formation
	+Mg							
Iron	Fe		0.3		0.2	0.3		Rusty colour, metallic taste, red staining
Manganese	Mn		0.05		0.04	0.05		Black or brown colour, black staining, bitter metallic taste
Sodium	Na				200	200		Salty taste
Sulphate	SO ₄		250		250			Salty taste
Zinc	Zn		5		1.5	1		Metallic taste

g No information available.

When present in very dilute concentrations, fluoride is not toxic, but when present in elevated concentrations or when consistently consumed, humans and animals can be plagued by chronic fluorosis. Skeletal and dental fluorosis can be debilitating or life threatening. The 1783-1784 Laki flood lava eruption in Iceland resulted in >60% of the grazing livestock to be decimated by the high fluoride in the surface water (Thordarson et al., 2003). Additionally, the effects of concentrated fluoride are harmful to plants.

Fluoride is not essential for plant growth, but it accumulates in plants when present. This can be an issue because concentrated Al, also leached from ash, is also considered toxic to plants, and in acidic environments Al and F bind to make toxic aluminofluoride complexes (Frogner Kockum et al., 2006). Small amounts of Cd, Cu, Se can all lead to liver or kidney damage, and As can damage skin and lead to increased cancer risk. High concentrations of Al and Mn from ash leachates can threaten the condition and health of flora and fauna as was seen in the 1991 and 2000 eruptions of Hekla, Iceland (Flaathen and Gislason, 2007). Mn is both an essential micronutrient and toxic when found in excessive concentrations (Millaleo et al., 2010). Although many ions released from the leaching of volcanic ash can be dangerous, there are also benefits of ash deposition.

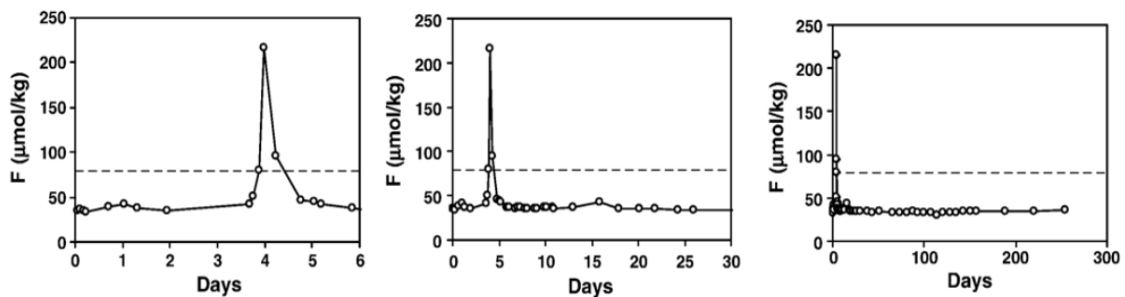


Figure 2. Fluoride concentration over 0-300 days in the Ytri-Rangá River after the 1991 eruption of Mt. Hekla, Iceland. Dashed horizontal lines represent the upper limit for safe drinking water (Flaathen and Gislason, 2007).

While some ions pose a short-term health hazard to flora and fauna, nutrients such as K, P, Mg, Fe, and other micronutrients derived from ash, can immediately fertilize soils and aide in long-term plant growth or short-term ocean fertilization. Increased Fe can lead to positive ecosystem effects such as ocean fertilization since it is a limiting nutrient in the

ocean (Frogner et al., 2001; Olgun et al., 2011; Durant et al., 2012; Browning et al., 2015). Due to aerosol deposition in the 2010 Eyjafjallajökull eruption there was significant dissolved Fe input into the Iceland Basin resulting in Fe fertilization. The eruption had the potential to increase the dissolved Fe in the water by >0.2 nM over an area of $570,000 \text{ km}^2$ (Achterberg et al., 2013). Cronin et al. (1998) studied how the volcanic ash from the 1995 and 1996 Ruapehu eruptions chemically affected soils in New Zealand. Beneficial elevated concentrations of S, Mg, K, and Se from the volcanic ash, were measured in the soils. These and other water soluble elements were readily available to be used by plants and can immediately influence soil fertility (Cronin et al., 1998). By understanding how volcanism harms or benefits the ecosystem, general characterizations can be made about ecosystem chemistry in distinctive volcanic regions.

4.2 Volcanic Ash Surface Area

Ash morphology, vesicles, particle size, and dust are all contributing factors of volcanic ash surface area, which in turn affects leaching rates. We define ash morphology as the unique shape of the individual ash particles including the external and internal topography. Ash morphology is partially controlled by bubbles in the melt which solidify into vesicles. While partial bubble imprints are seen on the outside of ash particles, some vesicles remain intact in the interior of the ash particles. The concentration and size of the bubbles in ash varies with composition and energetics. In volcanic ash particles, two populations of bubbles form. Pre-eruptive bubbles form deep within the conduit and grow due to nucleation during decompressive ascent within the conduit (Genareau et al., 2012; Toramaru, 2014). In some cases, a second nucleation produces another population of

bubbles, called syn-eruptive bubbles which are typically smaller and more abundant (Genareau et al., 2013; Toramaru, 2014). The Volcanic Explosivity Index (VEI) is a measure of the violence of a volcanic eruption (Newhall and Self, 1982) and can be related to bubble production. Lower VEI eruptions are characterized as less energetic with lesser decompression rates and produce shorter column heights, while eruptions with a higher VEI are more explosive and energetic and have taller column heights. As VEI increases, the bubbles' number density generally increases, and therefore surface area per mass increases. In general, mafic ash (e.g. basaltic), contains only pre-eruptive vesicles and has a lower surface area, compared to silicic ash, (e.g. rhyolitic), that can have both size populations of vesicles, increasing the surface area of the particle. Surface area can also vary within chemical composition. Kilauea and Eyjafjallajökull eruptions both produce basaltic ash, but their morphology varies significantly. Kilauea, which has low energetics, produces ash spherules, created by a small rotating melt droplet shaped by surface tension as it cooled. These contain only a few internal vesicles, minimizing the particle's surface area. However, Eyjafjallajökull ash was produced by mildly-explosive fragmentation resulting in irregularly shaped particles and pre-eruptive vesicles, resulting in a greater surface area.

Surface area per mass is strongly controlled by particle size. Smaller particles have greater surface area per mass and therefore, compared to the larger size population of ash, the smaller population has greater leaching potential on the environment. Volcanic dust is an endmember of particle size, in this study considered to be any particle $< 5 \mu\text{m}$ (Walker, 1981). Volcanic dust is likely created by fragmentation by milling and collision of ash particles in the upper conduit and eruptive column (Rose and Durant., 2009;

Langmann, 2013), although this has yet to be studied. Small fragments of ash ($< 5\mu\text{m}$) break off the larger particles and adhere to the surfaces of the ash particles. Similar processes can be seen in pebble abrasion during fluvial transport (Attal and Lavé, 2009). The dust increases the overall surface area of the sample. Dust is important because it can add a large amount of surface area and therefore increased leaching surfaces. Ash aggregates, the result of dust adhering onto the surface of ash particles, are bound by liquid-bonds, hydro-bonds, and electrostatic forces (Brown et al., 2012). Mueller et al. (2016) claim that the liquid binding agent (liquid-bonds) of ash aggregates are NaCl salt bridges. These salt bridges which form bonds allow aggregates to be preserved in the geologic record (Mueller et al., 2016). Hydro-bonds form in the upper troposphere as ice, which bind ash particles together, driving the aggregates to fall quickly out of the atmosphere. As humidity decreases, and there is less available water in the atmosphere, electrostatic forces play a larger role. It is not currently known if these forces can exist together or if are completely separate throughout the aggregate formation, deposition, and leaching process, although it is presumed that in this study the bonds are liquid NaCl bonds that partially dissolve over time. The balding effect (complete disaggregation) occurs on some ash particles, but not all, meaning that there are some bonds that remain intact throughout the week of experimental leaching. Although this is not the focus of this study, this continues to be an area of active research (Rose and Durant, 2011).

Surface area of ash is important to understand and quantify because it can allow us to correctly determine volcanic glass dissolution rates. The relation of mineral surface morphology on dissolution rates has been previously quantified (Jeschke and Dreybrodt, 2002), and can help determine which surface area measurement is more accurate. In the

present study, the surface areas are determined geometrically, which assumes perfect geometric shape, and by gas adsorption using BET analysis, which quantifies every surface including the internal vesicles. It is unknown which method better represents natural conditions. Therefore, it is important to compare both geometric and BET surfaces areas especially because they differ by a factor of ~ 100 , which changes the magnitude of the calculated dissolution rate. Previous specific surface areas of volcanic ash have been reported to range from 1-10 m^2/kg (Delmelle et al., 2005; Langmann, 2013), whereas geometric surface areas range from 0.005-0.07 m^2/kg . Wolff-Boenisch et al. (2004) determined that the geometric surface areas were superior over BET surface areas due to stronger linear regressions between the log of the measured dissolution rates and the silica content of the glasses for geometric normalized rates over the BET rates (Wolff-Boenisch et al., 2004), but Jeschke and Dreybrodt (2002), who studied the relation between mineral dissolution rates with surface morphology, demonstrated that the superior surface area measurement is dependent upon the surface morphology. If the entire surface contributes to leaching then BET surface area should be used when determining dissolution rates, but if there is a surface with deep ink bottle pores (which would trap water like batch experiments and not contribute to dissolution rates), it may be more accurate to use geometric surface area (Jeschke and Dreybrodt, 2002). Unlike a column leaching test (used in this experiment), which has a constant flow of source water, batch experiments do not have an in or out flow (ash and water are in a closed system) and tend to reach saturation state quickly.

It has not yet been determined whether the leaching water only interacts with the outer surface of the ash, in which case geometric surface area would be a better analog, or if

water travels into the interior vesicles of the ash. If the latter is true, BET normalized rates would likely be superior. The internal permeability of volcanic ash is challenging to quantify, and therefore it is unknown if the water can easily flow in and out of the vesicles or if some water gets trapped. The trapping would cause this system to act more like a batch experiment. There are still many unknowns about the interactions between water and ash particles, and this should continue to be studied.

4.3. *Geologic setting*

By comparing the geochemical trends of the ash leachates from diverse volcanoes, the expected water chemistry, resulting from future eruptions from various volcanoes, can be inferred. In this study, ash samples from volcanoes with recent eruptions in Alaska, Costa Rica, Iceland, and Hawaii are used.

Redoubt: Mount Redoubt (60.485°N 152.742°W) is a 3.1 km high glacier-covered stratovolcano in Lake Clark National Park, Alaska. It last erupted in March 2009, which was the first eruption since 1990. The eruption was categorized as a VEI 3, and produced low to intermediate-silica andesitic ash during the initial explosive phase of the eruption (Bull and Buurman, 2013). There was a shift in lava chemistry in early May 2009 to a high-silica andesite (Bull et al., 2013). This study uses the earliest explosive products which consist of low-silica andesites (<58 wt.% SiO₂) (Coombs et al., 2013). There are two rivers bordering the volcano; Drift River, to the north, and Crescent River, to the southwest, which provide means for testing the impact of volcanic ash leaching on the natural environment (Bull and Buurman, 2013). Bull and Buurman (2013) provide a

comprehensive overview of the eruption specifics, while Coombs et al. (2013) present an overview of the ash chemistry evolution.

Turrialba: Turrialba (10.025°N 83.767°W) is a 3.3 km stratovolcano in Costa Rica. It has been erupting intermittently since September 2016 and has continued emitting volcanic ash into March 2018. Geochemical analyses of the volcanic rocks from the region indicate a range of basaltic to dacitic lavas (Di Piazza et al., 2015). The eruption on May 20th, 2016, characterized as a VEI 3.1, produced an ash column that rose ~ 3 km above the crater. There have been health and safety concerns in the area, mostly due to high emissions of volcanic ash and gases (De Moor et al., 2016).

Eyjafjallajökull: Eyjafjallajökull (63.633°N 19.633°W) is a 1.7 km stratovolcano located in southern Iceland. It last erupted in April and May of 2010. Considered a VEI 4, it emitted far spreading ash that reached southern parts of Europe (Gudmundsson et al., 2012) and severely inhibited air travel (Fu et al., 2015). The eruption caused ecological and economic damage and the ash plume rose 9 km above sea level (Cioni et al., 2014). The closest rivers to Eyjafjallajökull, Markarfljótt and the Jo'kulsá í Solheima rivers, were both chemically affected by ash deposition (Bau et al., 2013). This is a promising confirmation that the ash deposition affected the nearby surface waters. Unfortunately, we cannot directly compare the results of our study to this study as Bau et al. (2013) were interested in the distribution of REE. A study completed after the eruption in 2010 measured the concentrations of Fe in the ocean and found that the water had been fertilized from the Fe leached from Eyjafjallajökull ash (Achterberg et al., 2013).

Kilauea: Kilauea (19.421°N 155.287°W) is a 1.2 km high shield volcano located on the Big Island of Hawaii. It is one the of longest active eruptions, which began in 1983. Kilauea eruptions are unique due to the “fragmentation” of low viscosity, basaltic melt, which is different from the violent fragmentation of more viscous melts (Parfitt, 1998). Due to the unique processes, Kilauea produces ash in the shapes of spheroids, hair, tears, breadcrust tears, scoria, and reticulate tephra; dependent upon the magma drop size as well as cooling and evolution time of the particle (Porritt et al., 2012). The morphology of the pyroclasts is driven by surface tension forces shaping the particles by viscous relaxation before the melt has had time to cool (Porritt et al., 2012). Hawaiian oral traditions have passed down the volcanic history of Kilauea which has helped in the understanding of the evolution of the volcano (Swanson, 2008).

5. Hypotheses

The goal of this project has been to quantify the relative influence of ash surface area and chemistry on dissolution rates of specific health and environmentally relevant species into surface and groundwater. This was completed using column leachate tests (CLTs) over a week-long time interval while quantifying surface area changes throughout the experiment. This has implications for how flora and fauna are affected geochemically by different types of eruptions.

I. Leaching rates are dependent on volcanic ash morphology and chemistry. The ash samples used in this study had a range of morphology and chemistry. Basaltic ash was expected to leach more metals per unit surface area than the andesitic ashes due to its mafic composition. The ash morphology which resulted in high surface area, i.e. dusty,

vesicular ash, was expected to initially leach at the fastest rate and produce the highest concentrations of ions, compared to samples with lower surface area. It was expected that the changing surface area was important to take into consideration when calculating dissolution rates over a time series. This was tested using CLT (including water chemistry analyses), SEM, and BET. In part, this hypothesis proved true.

II. As ash leaches surface ions into the environment, the surface area of volcanic ash changes throughout the leaching experiment. Surface area as a function of time can be measured during a leachate experiment analytically by BET and geometrically by SEM. Surface area was expected to initially decrease over the time series, but then increase. The presence of volcanic dust on a particle would increase surface area, but as the dust dissolved into the leachate, surface area was expected to decrease. As the leaching continues, it was expected that there would be some disaggregation of the particles, which would increase surface area. This was tested using SEM and BET. Surface area analysis demonstrated that although surface area did change throughout the leaching experiment, the explanation portion of this hypothesis proved false.

III. Upon ash deposition, water will be most influenced by volcanic leaching, and potentially unsafe for human or animal consumption, at the very beginning of leaching. The ash particles may have contained highly soluble metal salts that were expected to be rapidly released, when first in contact with water. Once near-surface metals were leached off the particle, interior metals would not have been easily leached. Therefore, the dissolved metal concentrations in the leachate would decrease and the system was expected to reach steady state. This initial dissolution of soluble salts into the water could create acids, creating a change in the pH record. The presence of small dust

particles on the ash surfaces was also expected to contribute to initial rapid leaching. This was tested with the CLT. This hypothesis tested true.

6. Methods

6.1 *Ash Samples*

Ash samples from Alaska (Redoubt), Costa Rica (Turrialba), Iceland (Eyjafjallajökull), and Hawaii (Kilauea) were used to test the hypotheses listed above. **Figure 3** shows Scanning Electron Microscope (SEM) images of representative populations of the four pristine ash samples prior to leaching. The bulk chemistry of the ash samples has been previously analyzed and published (Clague et al., 1999; Gislason et al., 2011; Coombs et al., 2013; Di Piazza et al., 2015; De Moor et al., 2016).

Redoubt: Ash from Mount Redoubt in Alaska was collected from a car windshield in March 2009. The ash was collected soon after being deposited and had not been altered by precipitation or other exposure to water. The low-silica andesitic ash is angular and has few pre-eruptive bubbles with some dust.

Turrialba: Andesitic ash from Turrialba in Costa Rica was collected on May 20th, 2016 by Gino Gonzalez. Turrialba is currently active and has produced many eruptive phases. The ash used in this study represents just one eruptive phase that began on May 20th, 2016. The ash is very dusty and has no obvious syn-eruptive bubbles. Another study collected volcanic glass in 2014 and found that the chemical composition of the ash was basaltic andesite to trachyandesite (an intermediate composition between trachyte and andesite) (De Moor et al., 2016); likely very similar to the composition of the glasses used

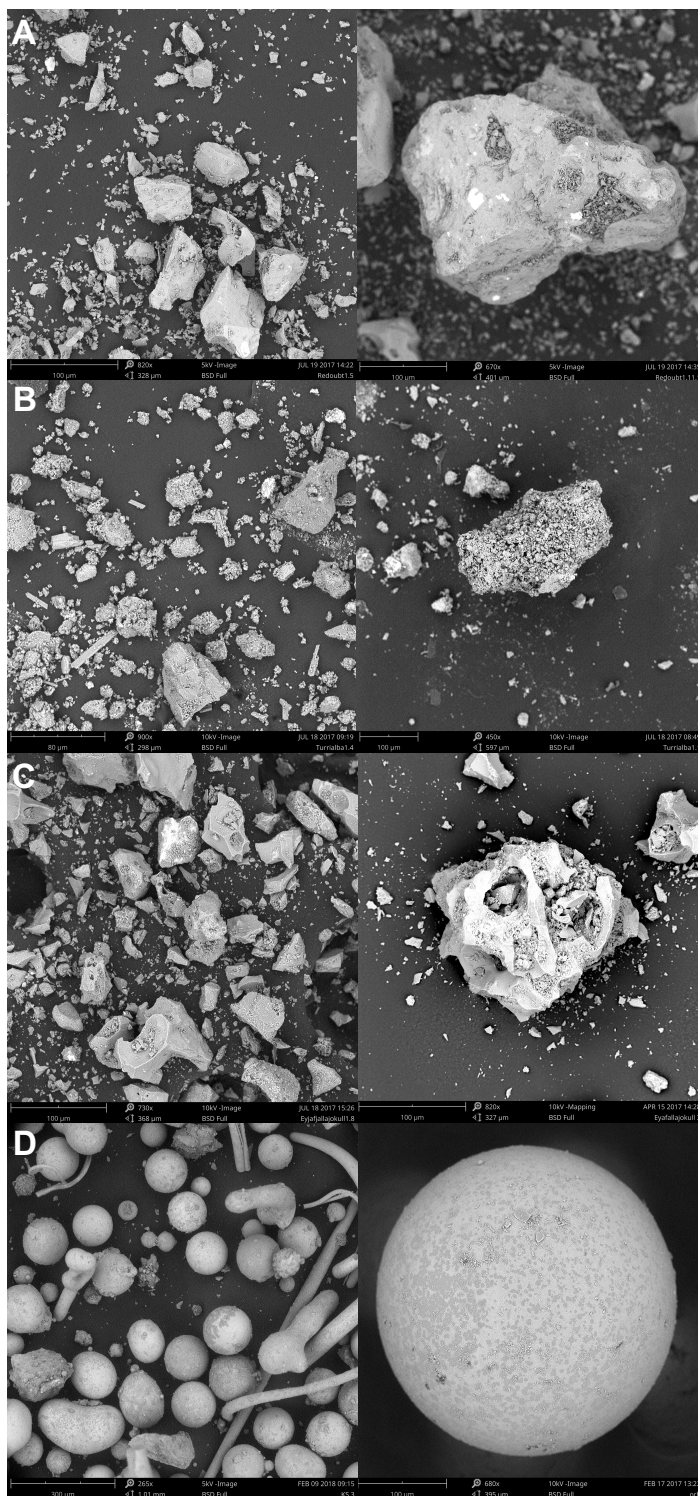


Figure 3. SEM images of the four pristine, unhydrated ash samples prior to leaching. Left column of images shows a larger population view while the right column shows one representative particle from each eruption: A) Redoubt ash, B) Turrialba ash, C) Eyjafjallajökull ash, and D) Kilauea ash.

in this study. The chemistry of volcanic rocks from Turrialba have been reported to range from basaltic andesite to dacite (Di Piazza et al., 2015).

Eyjafjallajökull: Basaltic ash from Eyjafjallajökull in Iceland was collected by Dr. Joe Licciardi of University of New Hampshire on May 6th, 2010, on the south side of the volcano, shortly after deposition, while the eruption was ongoing. The ash has a blocky to coarsely vesicular morphology (Cioni et al., 2014). Gislason et al. (2011) explained chemical differences of the two ash phases in the eruption; from the beginning explosive phase (producing explosive ash) in April to what they characterize as more “typical” ash later on in the eruption. The comparison of BET measurements provides evidence that the ash used in this study, which produced an initial specific surface area of 3.3 m²/g, is more similar to the explosive ash (surface area of 4.3 m²/g) versus the typical ash (surface area of 0.43 m²/g) in the 2011 study (Gislason et al., 2011).

Kilauea: Kilauea ash was collected in the winter and spring of 2017 by Dr. Don Swanson of HVO, ~ 470 meters from the vent in the lava lake in Halemaumau Crater. Kilauea produces basaltic Pele’s spherules, hair, tears, breadcrust tears, scoria, and reticulate tephra, dependent upon the magma drop size and cooling time of the particle (Porritt et al., 2012). In this study, Pele’s tears, spherules, and hairs are used for the leachate experimentation. There have been few detailed studies of Pele’s spheres, and there is much to be learned about the formation and characteristic of these unique pyroclasts. Glass spheres can be formed during various geophysical processes including lightning storms (Genareau et al., 2015) meteorite impacts, and low viscosity volcanic eruptions. Pele’s spheres have also been observed in andesitic volcanism, such as at Naka-dake crater. During active periods, Naka-dake crater, at Aso Volcano in southwest Japan,

occasionally erupts black ash formed by brittle fracturing of the top of the magma column and can produce Pele's hair and glass spheres from the underlying liquid magma (Ono et al., 1995). During the Aso eruptions, the spherules vary in color from yellow and silver gray in translucent glass with a thin devitrified skin, to black completely devitrified spherules. The spherules are most commonly associated with high temperature, low viscosity, basaltic explosive eruptions such as the current eruption at the Halemaumau crater, Kilauea volcano. The spherules are formed by rapid viscous relaxation due to surface tension before the spherules can cool and vitrify. Previous comprehensive studies mostly focused on the formation of larger tephra or Pele's tears, but Pele's spherules have been largely ignored in the literature. In this study, in addition to the leaching, a dozen spherules were mounted in epoxy and sanded approximately in half into order to reveal the interior of the ash.

6.2 Surface Area Analysis

Ash particles were imaged and characterized using a desktop Scanning Electron Microscope (SEM) at Lehigh University, and the long axis of the ash particles was measured using ImageJ software. No samples were sieved except for Kilauea, which originally had a much broader size distribution. The sizes were separated using a stainless-steel sieve (to minimize metal contamination (Witham et al., 2005; Jones and Gislason, 2008)) to include only particles $< 150 \mu\text{m}$. Tephra larger than this does not significantly contribute to short-term leaching in the surface water and soil. Samples were characterized based on morphology and dust on the ash surfaces. A small portion of each ash sample ($\sim 100\text{-}200$ particles, $> 5\mu\text{m}$) were measured after each leaching period (before leaching, post 1 hr, 8 hrs, 4 days, and 8 days). The particles were then binned based on

their sizes to measure size distribution. The changes in size distribution of the ash particles throughout the leaching experiment allowed the changes in geometric surface area to be correctly assessed. The geometric surface area (A_{geo}) was calculated using the area of an inscribed cube:

$$A_{geo} = 8r^2 \quad (1)$$

Where r is half of the long axis measured for an ash particle. The area was calculated for each measured ash particle then summed and divided by the sum of the total mass of all the ash particles. The mass of single ash particles was calculated using the volume of an inscribed circle:

$$V = \left(\frac{2}{\sqrt{3}}r\right)^3 \quad (2)$$

and then multiplying it by the glass density. For these calculations the bulk density of the Turrialba, Redoubt, and Eyjafjallajökull ash was assumed to be about 1500 kg/m^3 . This value was determined in previous studies (Moen and McLucas, 1980; Scott and McGimsey, 1994; Cronin et al., 1998; Stewart et al., 2006; Langmann, 2013) which presented a range of dry bulk densities of $500\text{-}3000 \text{ kg/m}^3$ depending on whether it was freshly fallen ash or compacted ashfall, if the chemistry was basaltic or andesitic, if there were crystals present, and the measurement of porosity. There was little to no crystallinity in the ash samples analyzed in this study, besides some adhered to the Turrialba ash. With the wide range of ash samples, it was decided that a density of 1500 kg/m^3 would be sufficient for calculations. Porosity varies between the Kilauea spherules with few internal vesicles and the more vesicular Eyjafjallajökull and Turrialba ash. Due

to the greater density of Kilauea, 2020 kg/m³ was used in calculations, a value previously determined as the average bulk density of Pele's spherules and tears (Porritt et al., 2012). In previous leaching studies (Wolff-Boenisch et al., 2004; Jones and Gislason, 2008) geometric surface area (Brantley et al., 1999; Gautier et al., 2001) was calculated by:

$$A_{geo} = \frac{6}{\rho \cdot d_{eff}} \quad (3)$$

Where ρ is the bulk density of the ash and d_{eff} is the effective particle diameter. The value in the numerator represents the assumption that the particles are smooth and spherical. The value for d_{eff} was calculated in previous studies under the assumption of a homogenous (flat) particle size distribution using (Tester et al., 1994):

$$d_{eff} = \frac{d_{max} - d_{min}}{\ln\left(\frac{d_{max}}{d_{min}}\right)} \quad (4)$$

where d_{max} and d_{min} represent the minimum and maximum particle size of the ash sample used for the leachate experimentation. This accepted calculation is not an accurate assumption of the geometric surface area since it assumes a homogeneous particle distribution, where there is an equal number of particles in each size bin. There are no natural samples of ash particles that are evenly distributed in terms of size. This may be a more appropriate assumption if the samples are milled and sieved prior to the leachate experiment. However, if samples are sieved and have a fixed maximum and minimum particle size, the calculation of d_{eff} cannot reflect the change in geometric surface area over time. These calculations also assume a spherical shape which minimizes the surface area of a particle, and does not consider any external (dust or other small surface particles) or internal (vesicles) complexities of the ash that significantly increases the

surface area available to leaching. While this may reasonably apply to Kilauea's perfect spherules, Kilauea is an end-member in terms of ash morphology. Most ash is angular, imperfect, vesicular, and dusty. The geometric shape of an inscribed cube, while still far from natural conditions, is a better geometric representation of ash particle than a sphere as assumed in previous studies, since it adds more surface area. This new way to calculate geometric surface area is recommended for future ash leachate studies.

The specific surface area of the ash particles before and throughout the leachate experiment was quantified using a Quantachrome multi-point Brunauer Emmett Teller (BET) method using Kr gas. Multi-point BET measurement quantifies the total surface area using Kr gas adsorption into the sample. The surface area is quantified five times, once before and four times throughout the leachate experiment. When the surface area, obtained by BET method, is used in the calculation of leaching rates it is assumed that all surfaces of the ash are available to be leached by the source water (Jeschke and Dreybrodt, 2002). Both surface areas are compared as a function of time and composition.

6.3 Ash Leachate Experimentation: CLT

To approximate steady state dissolution rates of volcanic ash in the natural environment, Column Leachate Tests (CLT) were completed to manipulate flow-through conditions (**Figure 4**). CLT were chosen for this study over batch tests, to allow the reaction to remain further from equilibrium as it would in nature, and most realistically recreate natural conditions. Both steady state (which exists in CLT) and chemical equilibrium (which is reached in batch tests) may produce unchanging concentrations, but during

chemical equilibrium the net reaction rate is approximately zero, so the rate of the forward

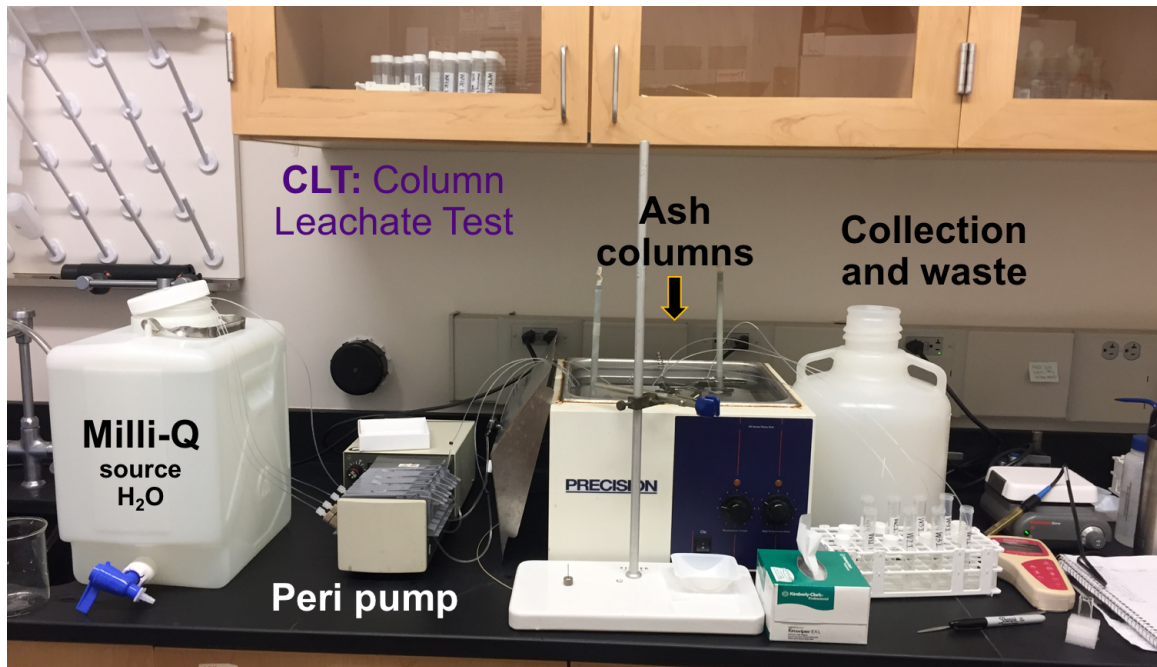


Figure 4. Column Leachate Tests (CLT) for week-long experiments. Milli-Q source water is pumped through four Teflon tubes at a constant flow rate using a peri pump. The water travels up through four identical columns packed with ash sitting vertically in a thermostatic water bath. The water then goes out to collection for analysis or to waste.

reaction is essentially equal to the rate of the backward reaction. Steady state exists at flow-through conditions (CLT) where the concentrations going into the system are the same as the concentrations going out (inflow = outflow). The constant flow of water in the CLT method prevents solution saturation state, and therefore chemical equilibrium, from being reached rapidly. This allows the reaction to take place far from equilibrium and therefore produce more accurate results (Taylor et al., 2000a). Approximately 4-6 grams of < 200 μ m ash particles, unsieved (besides Kilauea), were used from each eruption for analysis. The ash samples were leached according to standard CLT methods described in the literature (e.g. Taylor et al., 2000b; Witham et al., 2005; Jones and

Gislason, 2008; Chichester and Landsberger, 2012). The CLT were conducted in four identical BioSafe FEP Teflon tubes with an inner diameter of 0.46 cm and a length of 7.5 cm. Approximately 1-1.5 grams of dry ash was inserted into each column and mass was recorded. Milli-Q water was used as the leaching solute and the columns rested in a thermostatic water bath of $25 \pm 0.2^{\circ}\text{C}$. The Milli-Q source water passed through the columns at a rate of 0.28 ± 0.1 ml/min, based on previous CLT studies (Taylor and Lichte, 1980; Frogner et al., 2001; Witham et al., 2005; Chichester and Landsberger, 2012; Escudey et al., 2014; Cabre et al., 2016). Columns were positioned vertically so that source water entered through the bottom of the column allowing any air pockets to escape. Each column had a $2\text{ }\mu\text{m}$ FEP (Fluorinated Ethylene Propylene) Teflon filter at both the inlet and the outlet to prevent ash $> 2\text{ }\mu\text{m}$ from leaving the column. Four identical columns were set up simultaneously so that the experiment could be stopped at four different times. This allowed the ash to be characterized and surface area measured after 1 hour, 8 hours, 4 days, and 7 days. The leachate solution was collected every hour for the first 8 hours (2 samples in the first hour), then every 12 hours after that for 4 days, then every 24 hours for another 3 days. Replicate columns allowed for 2-3 water samples from the same time, allowing us to know the precision of the experiment.

6.4 Geochemical Analyses

After the column leachate runs were completed, the resulting water was prepared for geochemical analyses. Cation concentrations were determined by Inductively Coupled Plasma-Mass Spectrometry (ICP-MS). Ca, Mg, Na, Al, and Si were the main cations that have been previously measured by this technique in leaching studies (Armienta et al., 2002, Bagnato et al., 2011, Jones and Gislason, 2008). ICP-MS measures cation

concentrations by ionizing samples with a plasma using Argon gas. These samples pass through a quadrupole mass spectrometer which separate the masses of ions using electric currents. These signals are amplified, detected one at a time, and sent to a computer. Ion chromatography (IC) was used to measure anion concentrations, such as F, SO_4^{2-} and Cl. The IC measures anion concentrations by passing sample solutions through a chromatographic column where ions from the samples are absorbed onto the column. An eluent (NaOH), which is an ion extraction liquid, is passed through the column and separates the absorbed ions from the column. The unique retention times of the anions determine the ionic concentrations in the samples. Once the geochemical concentrations were collected, the concentrations of the leachates from each eruption were compared.

7. Results

7.1 Surface Area

Over the leachate experiment, the surface area of volcanic ash changed at different rates over the week depending on the chemistry of the ash (**Figure 5**). For all samples, BET measured specific surface areas were 2 to 3 orders of magnitude larger than geometric surface areas, which will be explained in the following section. For the more silicic ashes (andesitic/ andesitic-basaltic) ashes such as Redoubt and Turrialba, the BET surface areas increased then gradually decreased, whereas for the basaltic ashes, Kilauea and Eyjafjallajökull decreased then gradually increased (**Figure 6**).

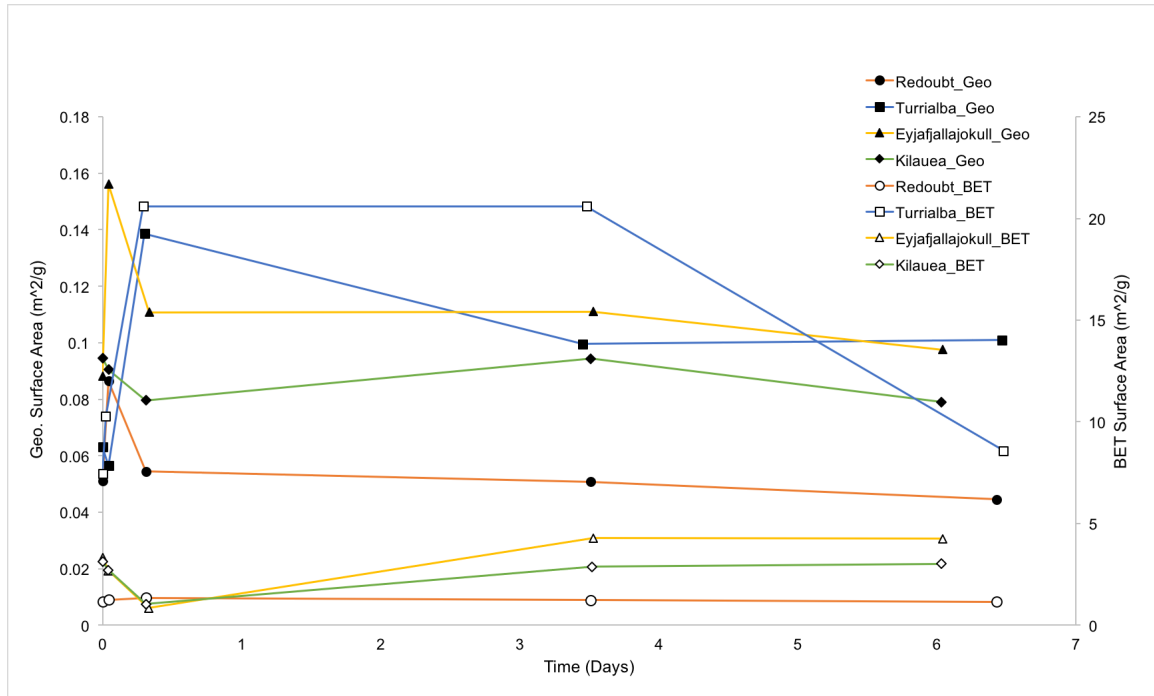


Figure 5. Geometric and BET surface area data for all ash samples throughout the leaching experiment, measured in m^2/g . Geometric surface area is plotted on the primary (left) Y-axis and BET surface area is plotted on the secondary (right) Y-axis, and time of the leaching experiment is on the X-axis. The observed trends represent the disaggregation, dissolution, and weathering of the ash particles.

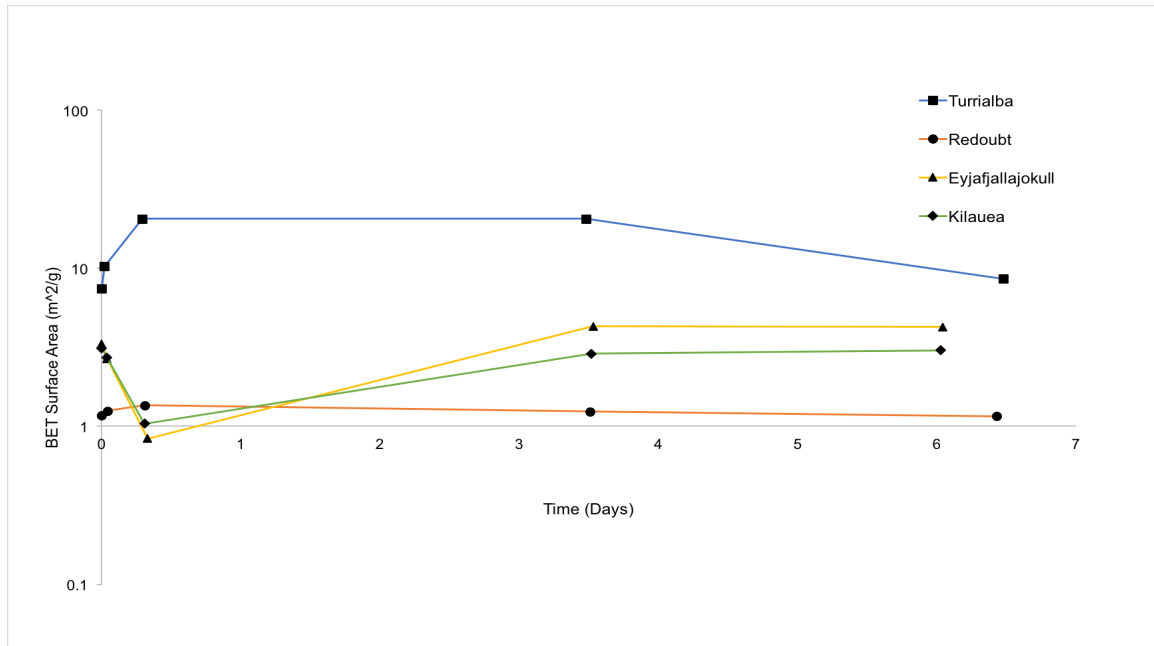


Figure 6. BET surface areas for all ash samples over one week measured in m^2/g . Time is plotted in days. Andesitic ashes (Turrialba & Redoubt) show an initial increasing trend in surface area then gradual decrease, representing disaggregation and dissolution of the ash whereas basaltic ashes (Eyjafjallajökull & Kilauea) show an initial decrease and then gradual increase in surface area, representing dissolution and then weathering of the ash particles.

The surface area of Redoubt ash increased from $1.17 \text{ m}^2/\text{g}$ to $1.35 \text{ m}^2/\text{g}$ over the first eight hours, then fell to $1.16 \text{ m}^2/\text{g}$ over the rest of the week. Although there is a maximum surface area between the start of the experiment and four days later, the maximum point may be greater than $1.35 \text{ m}^2/\text{g}$, reached at some point between measurement times.

Turrialba presented a similar trend increasing from $7.46 \text{ m}^2/\text{g}$ to $20.6 \text{ m}^2/\text{g}$ over 8 hours, then decreased to $8.59 \text{ m}^2/\text{g}$ by the end of the leaching experiment. There is likely a surface area maximum that was not recorded between 8 hours and 4 days of the experiment. Previous studies that measured specific surface area of ash reported a range of $< 2 \text{ m}^2/\text{g}$ up to $10 \text{ m}^2/\text{g}$ (Delmelle et al., 2005; Langmann, 2013). Our results show that Turrialba measured twice this previous maximum, which may reflect the exceptionally large amount of dust and potentially small vesicles present in the analyzed ash. For the basaltic ashes, Eyjafjallajökull and Kilauea, the surface area initially decreased and then increased over the week-long experiment. Eyjafjallajökull decreased from $3.33 \text{ m}^2/\text{g}$ to $0.83 \text{ m}^2/\text{g}$ over the first 8 hours then increased to $4.25 \text{ m}^2/\text{g}$ over the rest of the experiment. Kilauea ash had a similar trend of a decrease of $3.12 \text{ m}^2/\text{g}$ to $1.04 \text{ m}^2/\text{g}$ over the first 8 hours then increased to $3.02 \text{ m}^2/\text{g}$ over the rest of the seven-day experiment.

The trend of seen with the Redoubt and Turrialba ashes with surface area initially increasing, then decreasing, is also seen with geometrically calculated surface areas. Measured particle size distribution allowed for a visible representation of how the population of particles was changing over time (**Figure 7**).

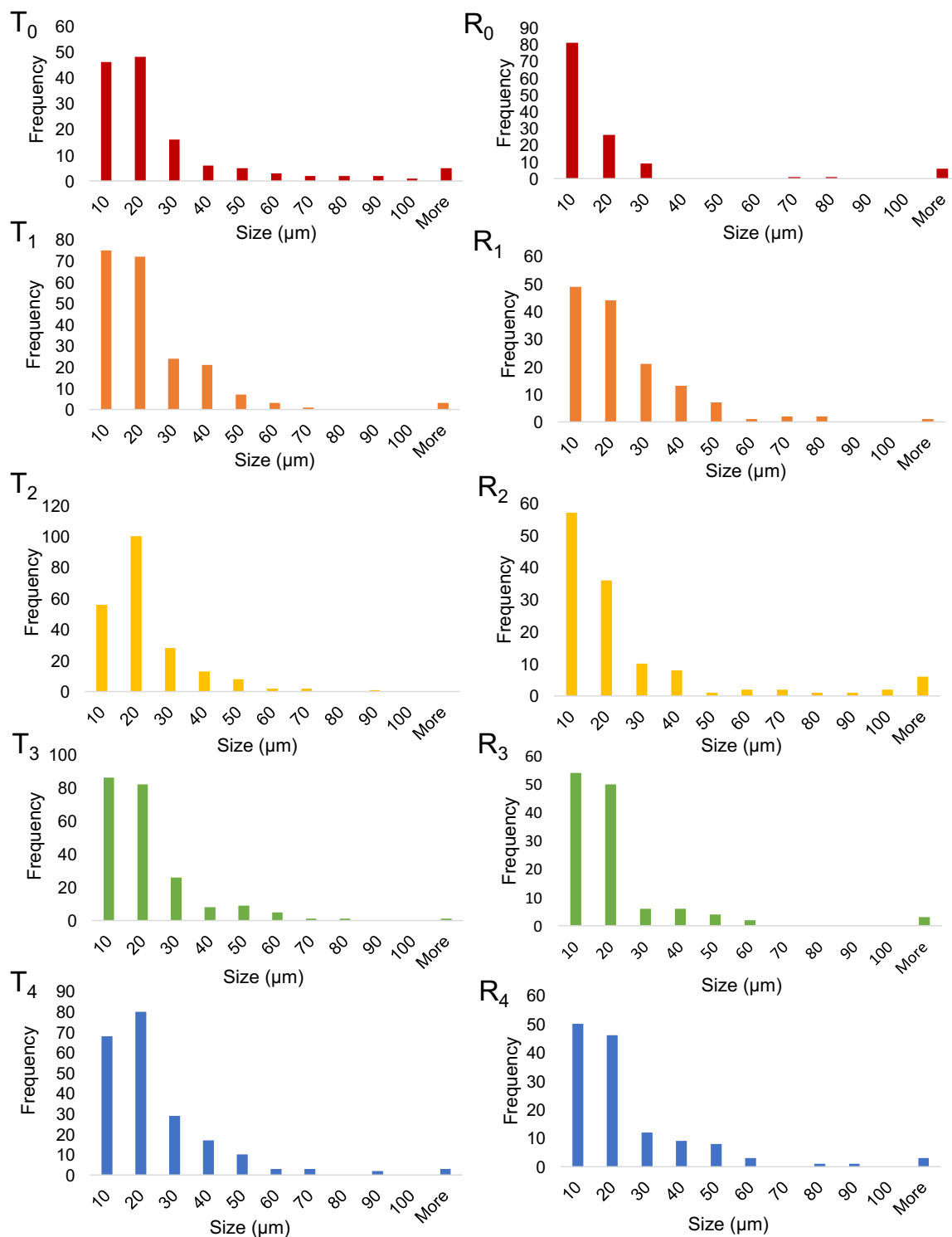


Figure 7. Measured particle size distribution, using the SEM and Image J, of Turrialba (left column) and Redoubt (right column) ash over one week. Frequency of particles is plotted on the Y-axis and binned sizes of the particles in μm is on the X-axis. Subscripts equal the time that the ashes were leached for. 0: Initial ash before leachate test, 1: Post 1 hour of leaching, 2: Post 8 hours of leaching, 3: Post 4 days of leaching, 4: Post 7 days of leaching. Greatest number density of particles is $< 20 \mu\text{m}$ for both populations.

This aided in calculating geometric surface areas. For most samples, there was an initial increase in geometric surface area over the first 1-8 hours of the experiment (**Figure 8**).

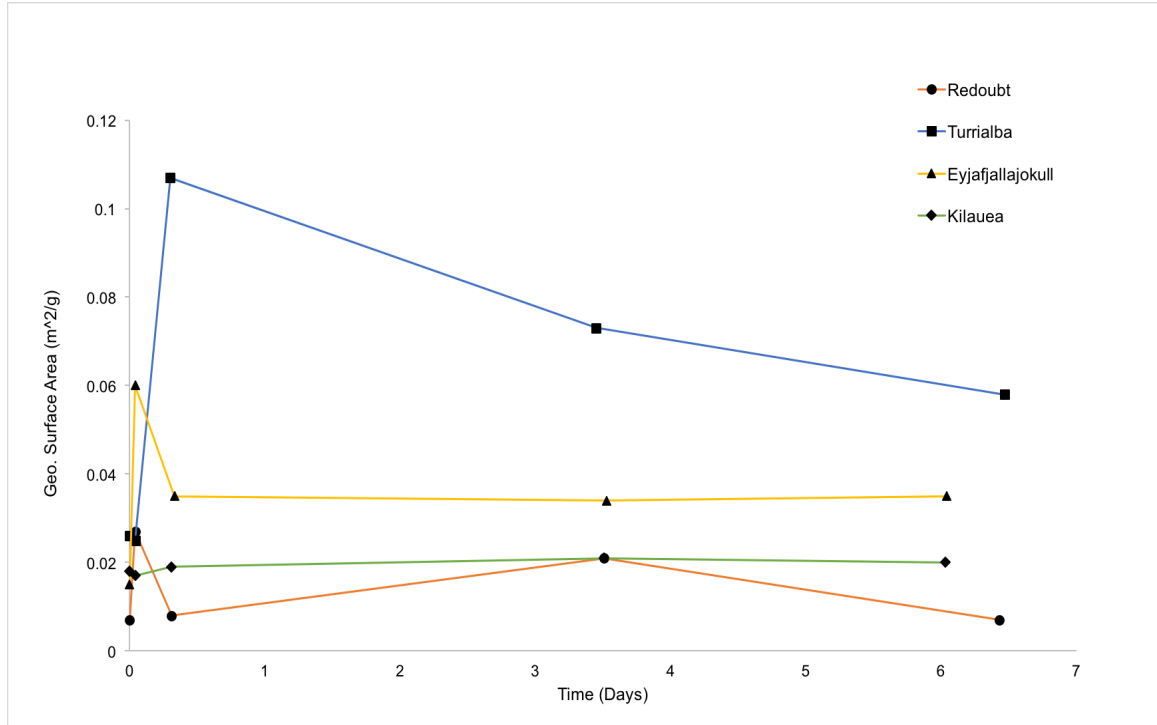


Figure 8. Calculated geometric surface areas for all ash samples over one week measured in m^2/g . Time is plotted in days. Geometric surface area only incorporates particles $> 5 \mu\text{m}$. All ashes show an initial increasing trend in surface area then gradual decrease over the remainder of the leaching experiment. This trend represents the disaggregation and dissolution of the ashes.

Turrialba ash surface area increased from $0.026 \text{ m}^2/\text{g}$ to $0.11 \text{ m}^2/\text{g}$ over the first 8 hours, then decreased to $0.058 \text{ m}^2/\text{g}$ over the week. Redoubt increased from $0.007 \text{ m}^2/\text{g}$ to $0.027 \text{ m}^2/\text{g}$ over the first hour, then decreased to $0.008 \text{ m}^2/\text{g}$ over the next 8 hours. The surface area of Redoubt ash increased to $0.021 \text{ m}^2/\text{g}$ at 4 days before decreasing to $0.007 \text{ m}^2/\text{g}$ by the end. Eyjafjallajökull increased from $0.015 \text{ m}^2/\text{g}$ to $0.06 \text{ m}^2/\text{g}$ over the first hour before decreasing to $0.035 \text{ m}^2/\text{g}$ by the end of the experiment. The Kilauea ash did not share the same trend as the other samples as its surface area varied only by $0.003 \text{ m}^2/\text{g}$ over the

leaching experiment, most likely due to its unique morphology, ranging from 0.013 m²/g to 0.016 m²/g. The spherules do not have angular edges or significant dust, minimizing readily dissolvable surfaces with a favorable hydrodynamic shape where water can easily flow over and around the particles.

Imagery from the SEM clearly reveals particle alteration throughout the leaching experiment. Turrialba is a useful sample to understand the effect of surface area on dissolution rates since there is a significant change in the specific surface area over the leaching experiment (**Figure 9**).

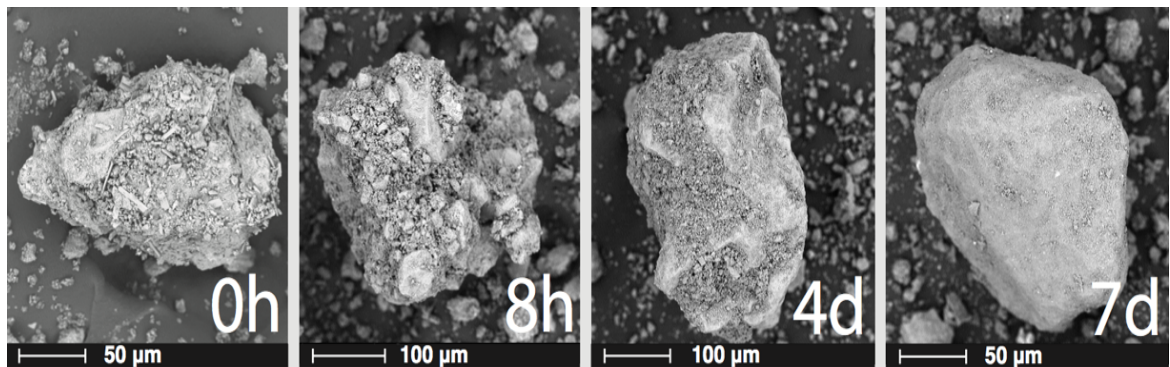


Figure 9. SEM images of Turrialba ash throughout the leaching experiment at four different time intervals; initially, post 8 hours, post 4 days, and post 7 days. This time series demonstrates the balding effect which consists of the disaggregation and dissolution of the dust particles into the leachate.

Figure 9 shows SEM images of Turrialba particles throughout the leaching experiment. The first image shows an unhydrated ash particle before leaching. The surface of the ash particle is covered in dust. The second image shows a particle after it had been leached for eight hours. The small dusty pieces are less apparent and some of the surface complexities, such as small ash nodules that are likely held on by NaCl bonds, are revealed since the ash has begun to disaggregate. The process of disaggregation removes some of the dust from the ash surface and increases overall surface area per mass. After

four days, some bare surfaces were revealed, while smaller particles lingered in the crevasses. After seven days, some surfaces were bare of the dust, decreasing the overall surface area per mass. This “balding” effect that occurred in this SEM time series was not seen with all particles, but was prevalent enough to explain the measured and calculated trends in surface area. Once the ash particles were stripped of the surface dust (balding), overall surface area decreased. This pattern also occurs with Redoubt and Eyjafjallajökull ash samples, but Turrialba is the best model to visualize the change in surface area due to its high dust content. In comparison, Pele’s spherules from Kilauea weathered uniquely. Some of the outer shells of the spherules fractured in a mud-crack pattern (**Figure 10**). Independent of ash chemistry and technique, as the volcanic ash leached into the environment, surface area of the ash increased initially gradually decreased over the week, and eventually increased (seen with the BET surface area of Eyjafjallajökull and Kilauea).

7.2 Chemistry

Over the leachate experiment, the ash from all analyzed eruptions released halogens, sulfate, nutrients, and heavy metals into the source water. The mass concentrations of SO_4^{2-} , Cl, and F from this study, aligned well with the chemistry from other studies (**Figure 11**). The collected and sampled leachate water was free from any particles; meaning that dust smaller than the 2 μm frit, may have dissolved into the outlet solution. The greatest initial concentrations of ions were released into the Milli-Q water within the first half hour of the leachate experiment, including SO_4^{2-} ($\leq 38900 \mu\text{mol/kg}$), Mg ($\leq 19400 \mu\text{mol/kg}$), Al ($\leq 14900 \mu\text{mol/kg}$), Ca ($\leq 13500 \mu\text{mol/kg}$), F ($\leq 4050 \mu\text{mol/kg}$), Na ($\leq 3010 \mu\text{mol/kg}$), and Cl ($\leq 3010 \mu\text{mol/kg}$) (**Figure 12**). Figure 12 shows the

concentration, flow rate data, as well as the dissolution rates for the major elements released separated by eruption.

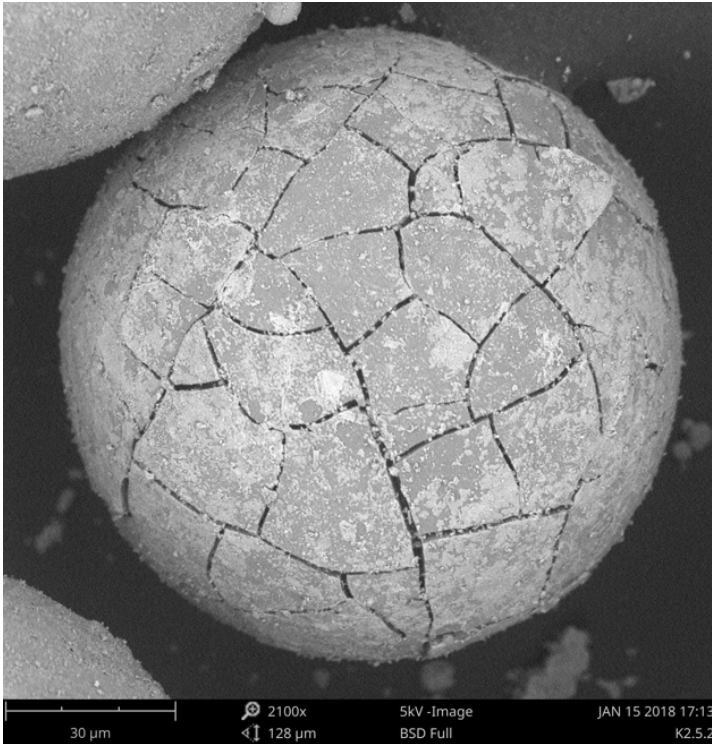


Figure 10. SEM image of a Pele's sphere after it had been leached for 1 hour. This image demonstrates the mud-crack weathering pattern, unique to these spherules. While this pattern was commonly seen in the ash after leaching, it was only observed on a small population of particles after the entire week of leaching.

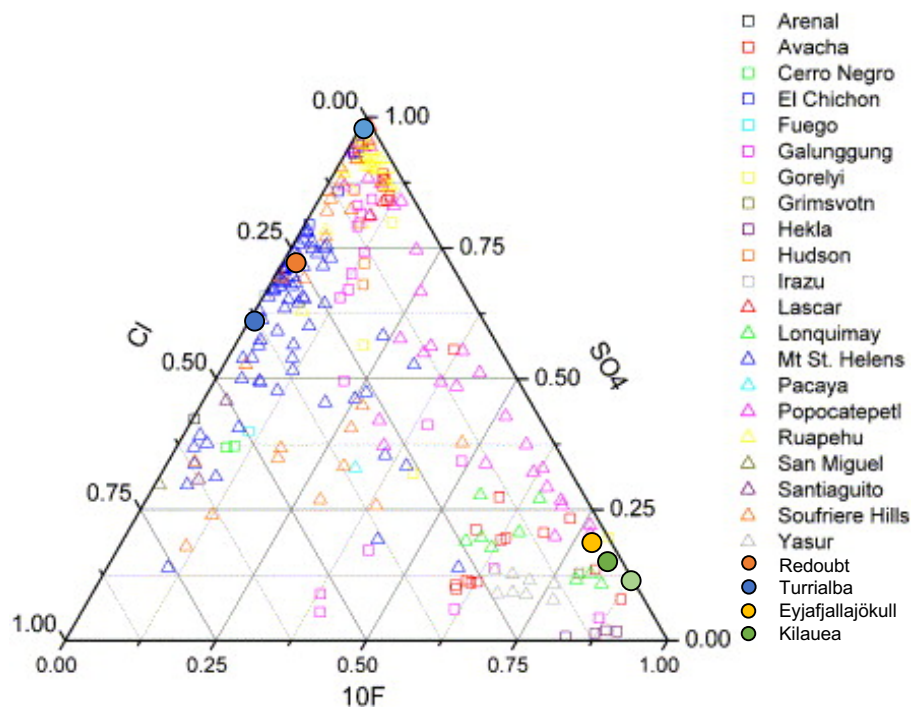
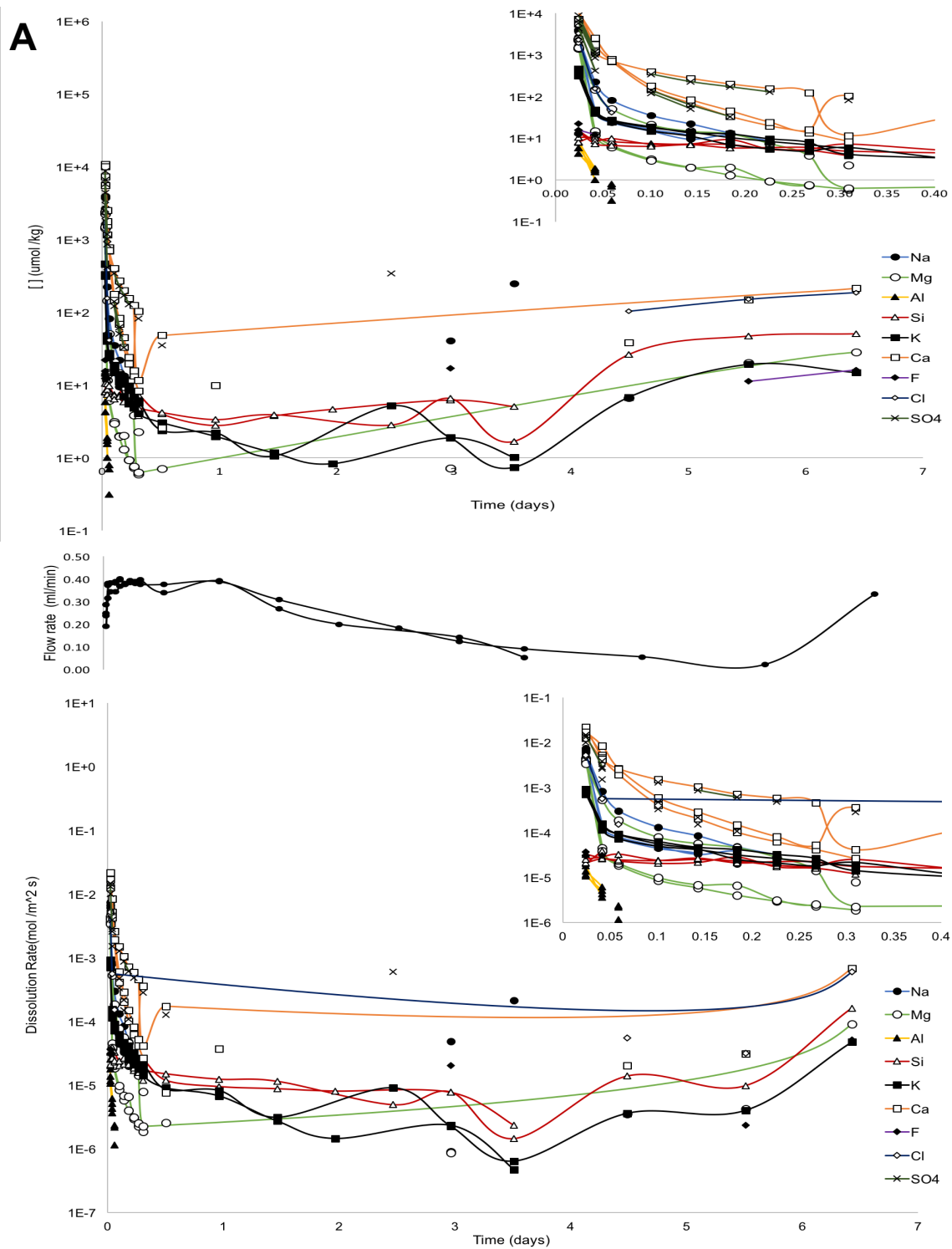
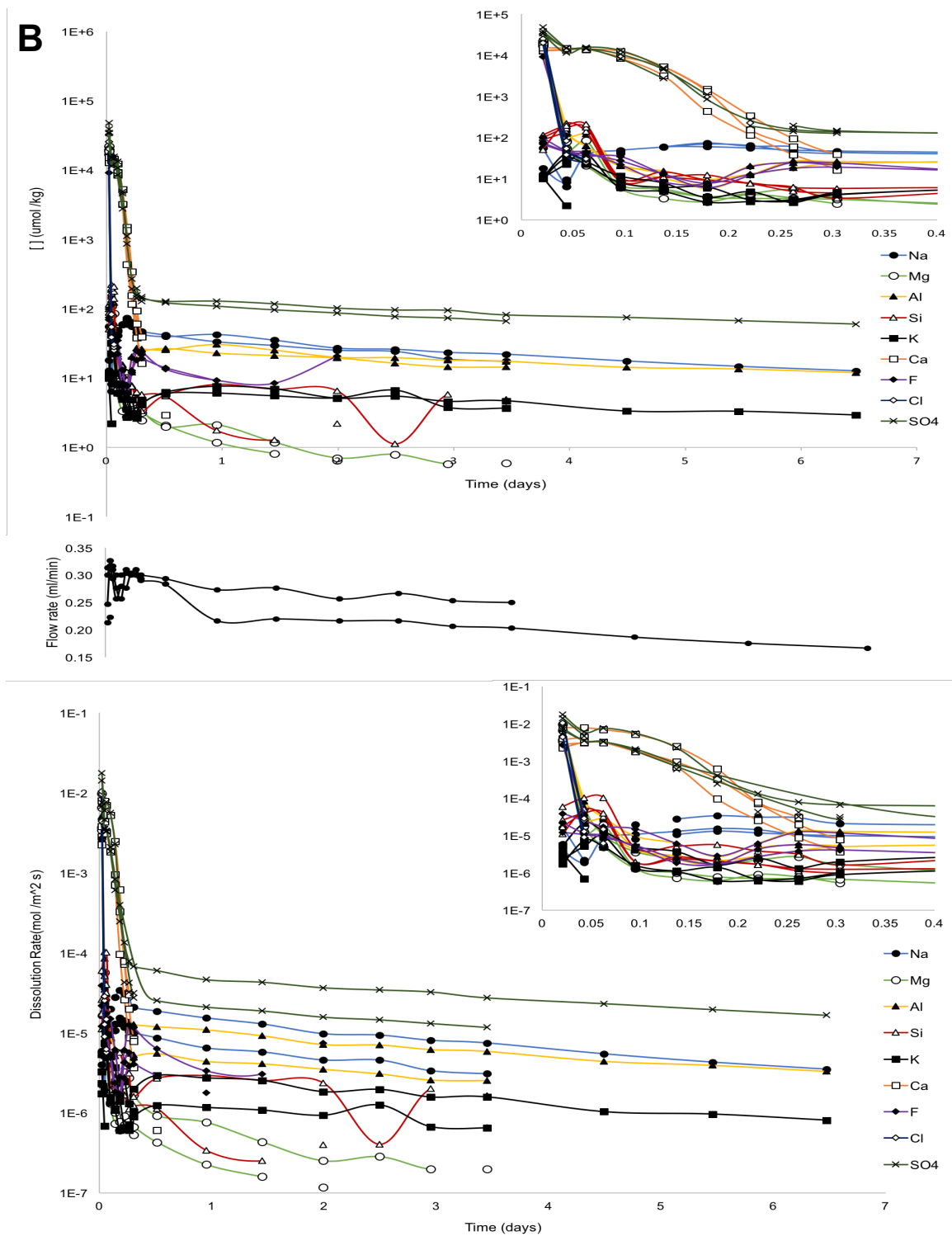
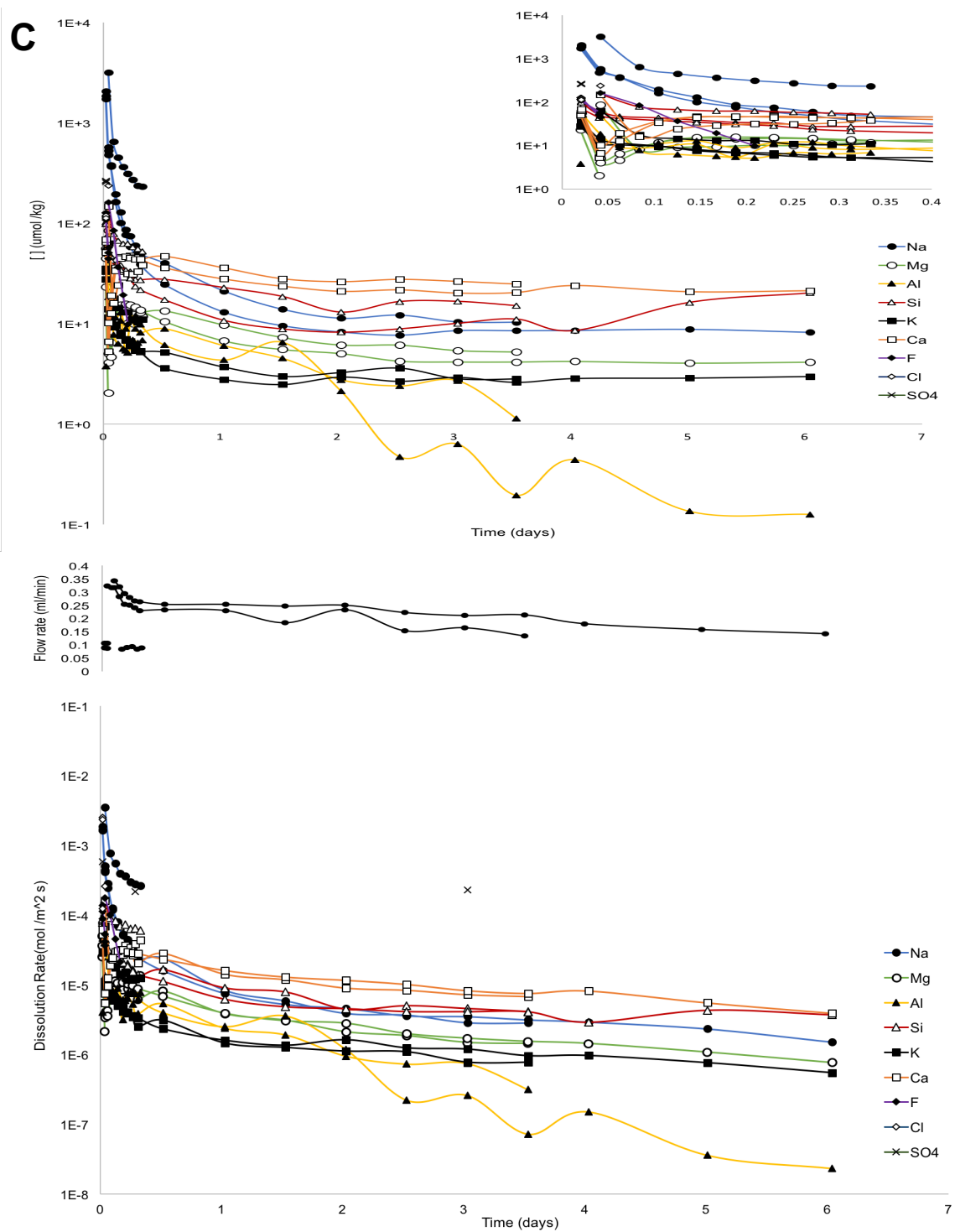


Figure 11. Ternary diagram from Witham et al. (2005) showing the relative SO_4^{2-} , Cl, and F ($\times 10$) absorbed mass concentrations from a compilation of ash leachate analyses, including the current study. Points from this ash leachate analysis represent the chemistry after the initial 30 minutes of leaching. Light blue and light green dots represent the chemistry of the leachate after an hour for Turrialba and Kilauea respectively.







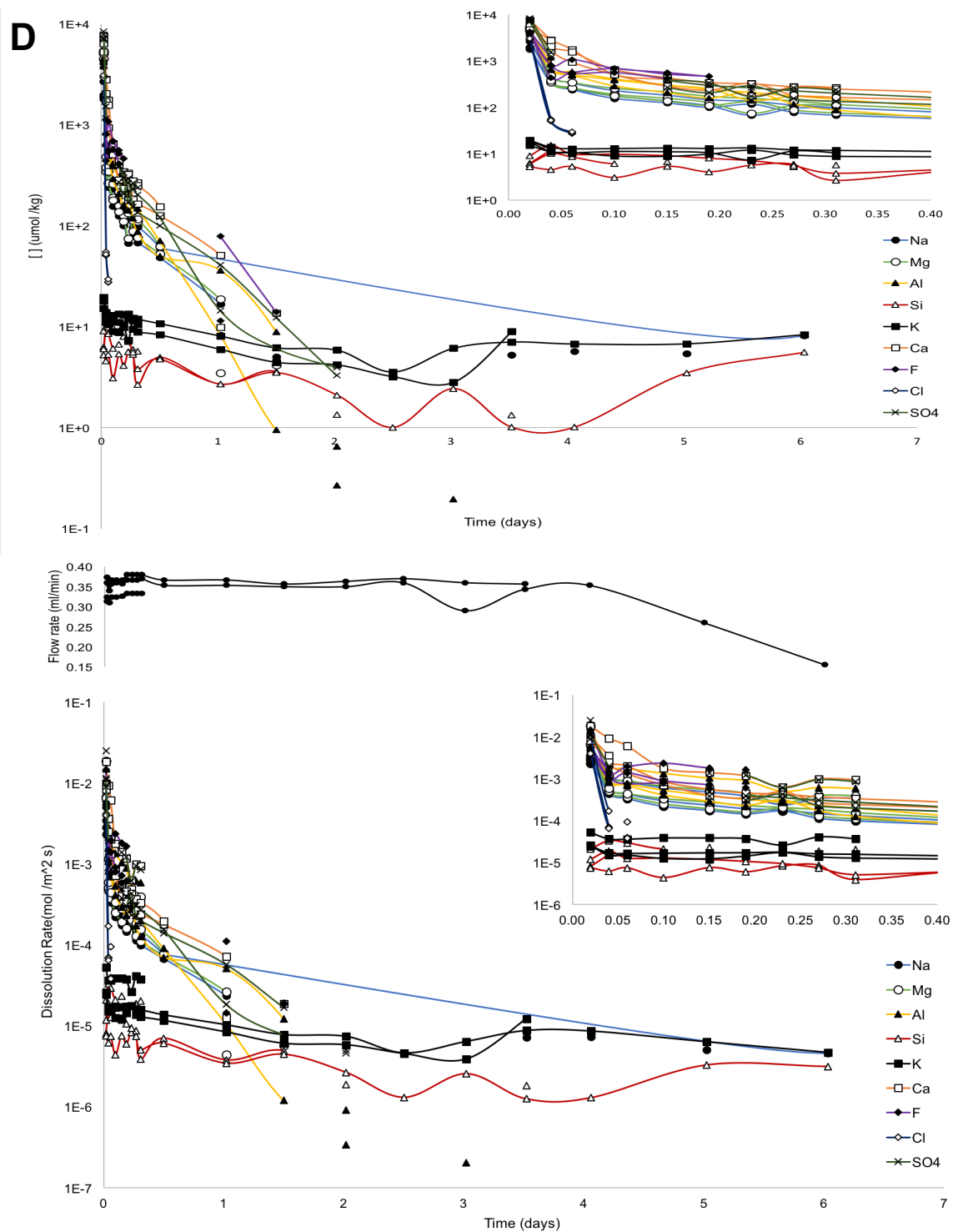


Figure 12. Concentrations ($\mu\text{mol/kg}$), flow rates (mL/min), and dissolution rates ($\text{mol/m}^2 \text{s}$) of major elements from all volcanic ash samples against time (days) over the week-long experiment. A) Redoubt, B) Turrialba, C) Eyjafjallajökull, and D) Kilauea. Rapid initial decay in

concentration and dissolution rate seen in all samples. Two chemical populations seen in Kilauea and potentially in Turrialba.

The initial leachate samples (i.e. volcanic ash with source water), revealed an initial decrease in pH then a slight increase over the rest of the experiment (**Figure 13**).

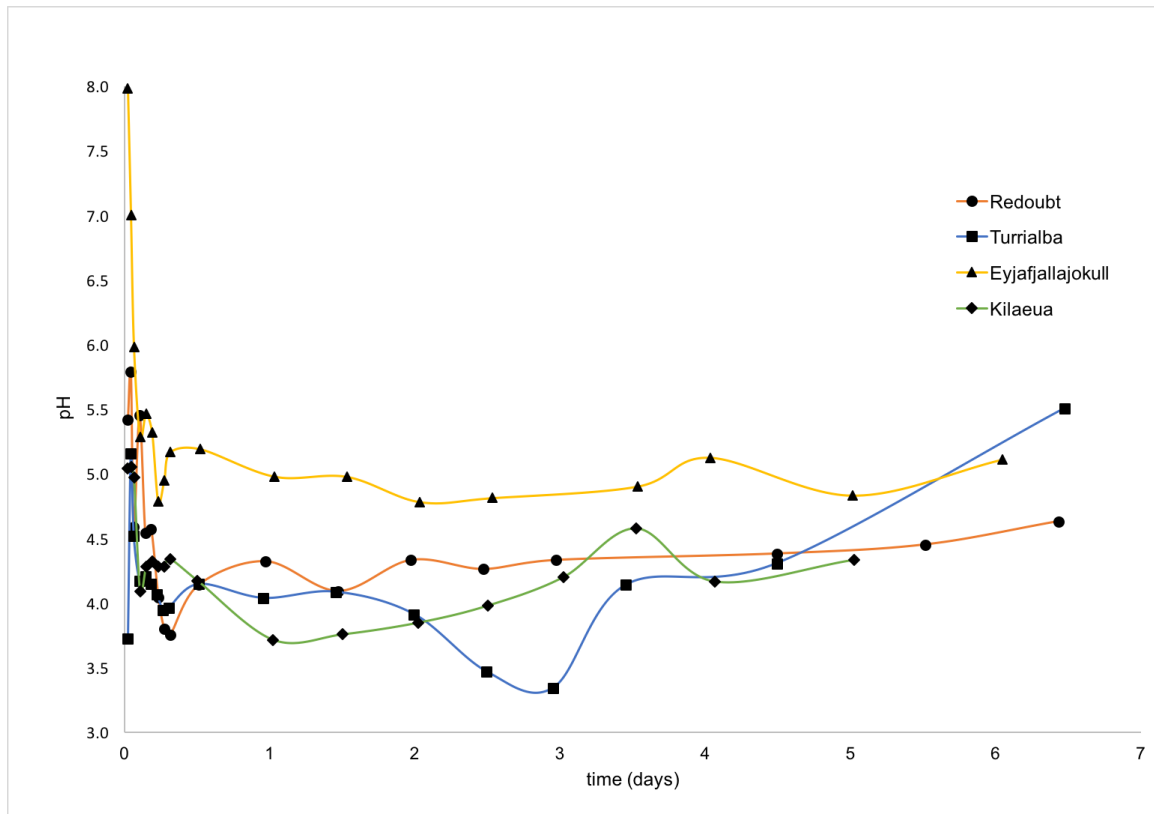


Figure 13. pH of volcanic ash leachates for all samples over the week-long leaching experiment plotted against time in days. There is an initial decrease in all samples and then a gradual increase towards a neutral pH towards the end of the week. This provides evidence for the dissolution of the acid magmatic gasses which initially dissociate to lower pH.

Eyjafjallajökull presented the greatest change in pH over the time series. Beginning at a pH of 8.0 before plunging to a pH of 4.8 after 5 hours. Turrialba dropped to the lowest pH of the samples at 3.3 after 3 days but then increased to 5.5. With slight differences in timing, trends in pH are similar for Kilauea and Redoubt.

Far from equilibrium steady-state dissolution rates of halogens, sulfate, and major nutrients were calculated as a function of time using BET surface areas using:

$$r = \frac{C \cdot f_r}{A \cdot m} \quad (5)$$

where C is the aqueous species concentration of the outlet solution, f_r is the flow rate of the system, A is the specific or geometric surface area of the volcanic ash and m is the initial mass of the sample (Wolff-Boenisch et al., 2004). In this study, dissolution rates were calculated using changing BET specific surface area measurements. Most studies assume a non-changing surface area, but we hope to improve the calculation of these rates by using the evolving surface area over the leaching experiment. Regardless of the ion, dissolution rate had an initial rapid decay. Some ions reached steady state over the week whereas others did not (e.g. Al in the Eyjafjallajökull leaching record) (**Figure 12**). Some fluctuations in the dissolution rates over the week can be attributed to changes in flow rate. The changing flow rate did not have a significant influence on the dissolution rates because flow rate varied within an order of magnitude while dissolution rate varied over multiple orders of magnitude. The fastest dissolution rates of various ions were found in the Turrialba samples, which had the greatest surface area. Ash with the highest surface areas, and most dust, were expected to have the greatest number of leaching surfaces and therefore the highest dissolution rates. Taking changing surface area into consideration when calculating dissolution rates is of greater importance for dusty samples, which have a broader size distribution of particles. Note: after the leaching experiment had been completed for some time the leached Turrialba water precipitated gypsum (**Appendix C**).

The range of heavy metals that are released into the environment by leaching of ash can be detrimental to human and animal health. Initial accumulated concentrations after one hour were calculated and are shown in **Figure 14**. Initial accumulations (after 1-hour) of F ($\leq 2430 \mu\text{mol/kg}$), Cu ($\leq 40.4 \mu\text{mol/kg}$), Cd ($\leq 3.83 \mu\text{mol/kg}$), Cr ($\leq 0.96 \mu\text{mol/kg}$), Se ($\leq 0.20 \mu\text{mol/kg}$), and As ($\leq 0.13 \mu\text{mol/kg}$) are the main elements of health concern for these ashes. Some of the accumulated concentrations are above the World Health Organization (WHO) standards for safe drinking water (**Figure 14**). Kilauea ash, the basaltic chemical endmember, and Turrialba ash, the surface area endmember are consistently the ashes leaching the highest concentrations of harmful species.

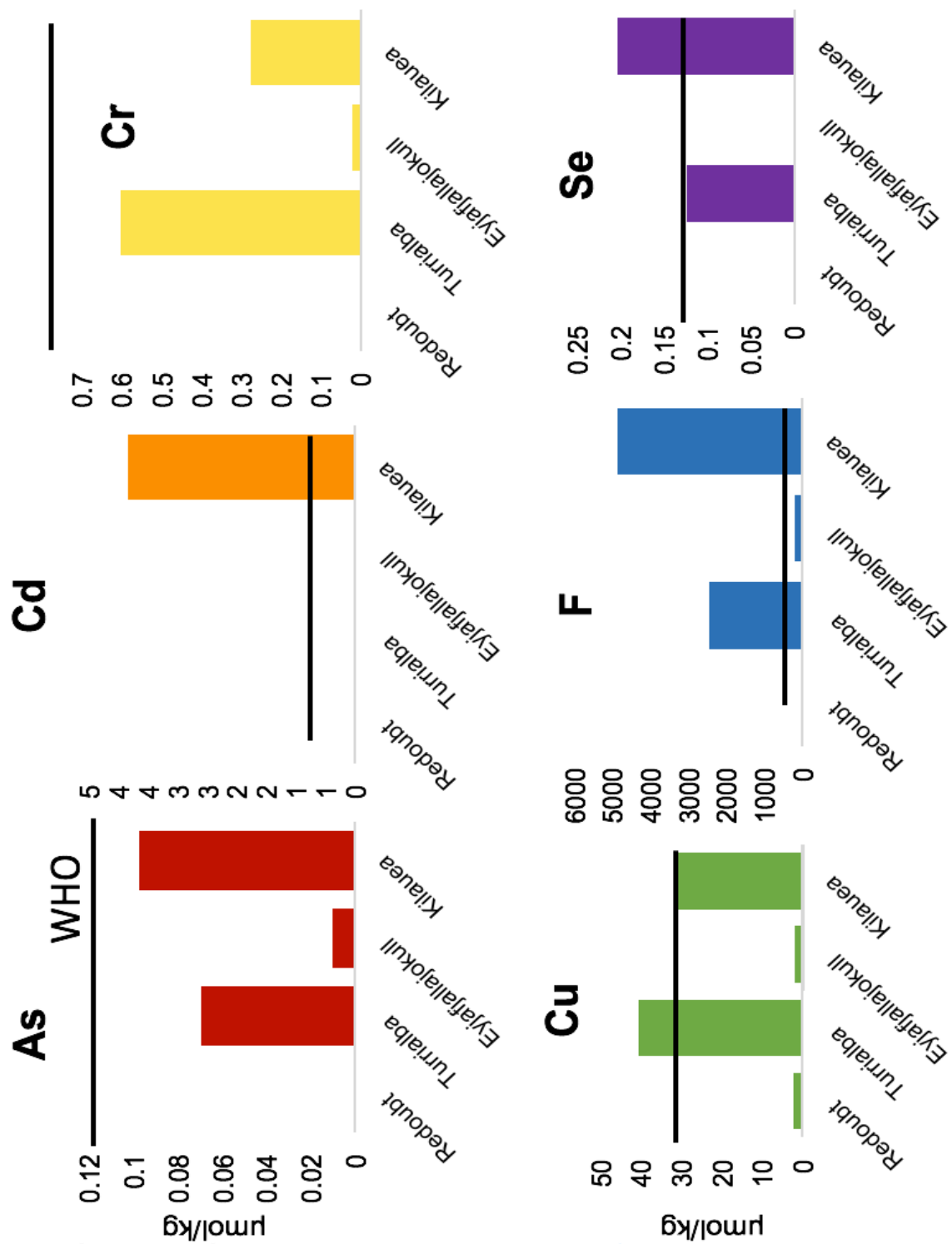


Figure 14. Accumulated concentrations ($\mu\text{mol/kg}$) of health-relevant elements (As, Cd, Cr, Cu, F, and Se) after 1-hour of leaching. The solid black line represents the WHO upper limit for safe drinking water standards. Kilauea, the chemical (basaltic) endmember, and Turrialba, the surface area endmember, consistently leach the highest concentrations.

The WHO standard for fluoride in drinking water is 79 $\mu\text{mol/kg}$. The accumulated concentration of F exceeded the safe drinking standards by all eruptions except Redoubt (**Figure 15**).

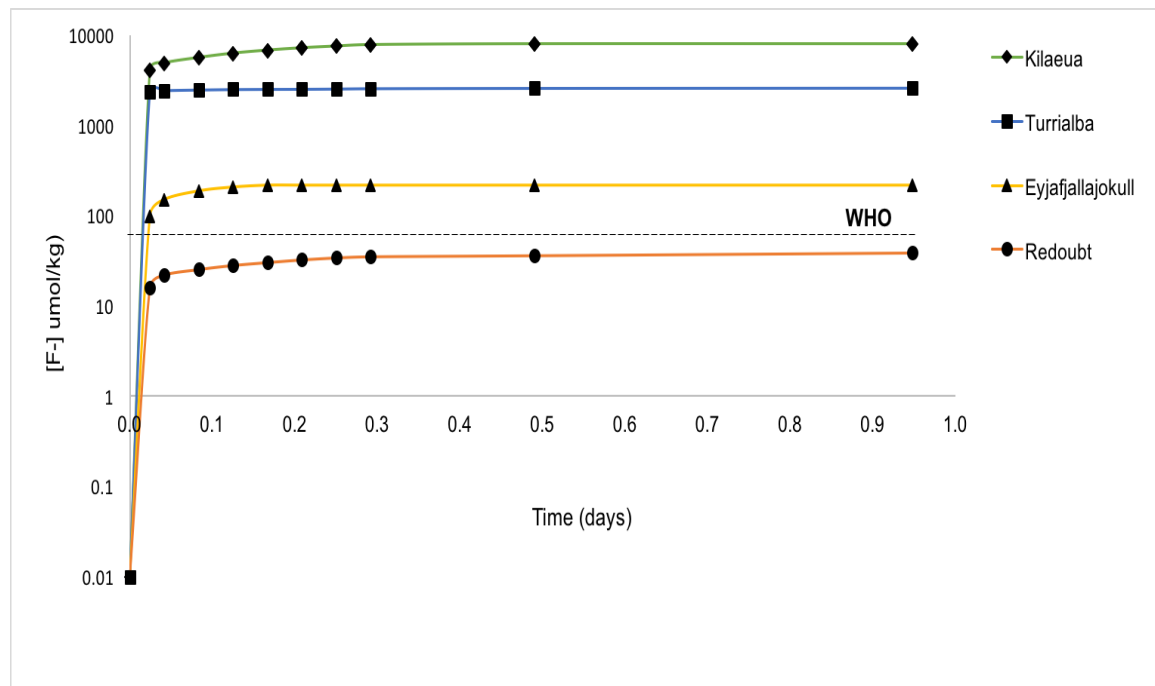


Figure 15. Accumulated fluoride concentrations ($\mu\text{mol/kg}$) over the first day of the leaching experiment for all ash samples. The WHO dashed-line marks the upper limit for safe drinking water. Kilauea, the chemical (basaltic) endmember, and Turrialba, the surface area endmember, leach the highest concentration of fluoride.

Kilauea has the greatest accumulation, followed by Turrialba, Eyjafjallajökull, then Redoubt. The highest concentrations are once again from the chemical and surface area endmembers, Kilauea and Turrialba respectively. Pure basaltic ash (Kilauea) released a higher amount of fluoride than andesitic/ andesitic-basaltic ash.

7.3 *Pele's Spheres*

A dozen spherules from Kilauea were mounted in epoxy and polished to expose the interiors of the spherules (**Figure 16**).

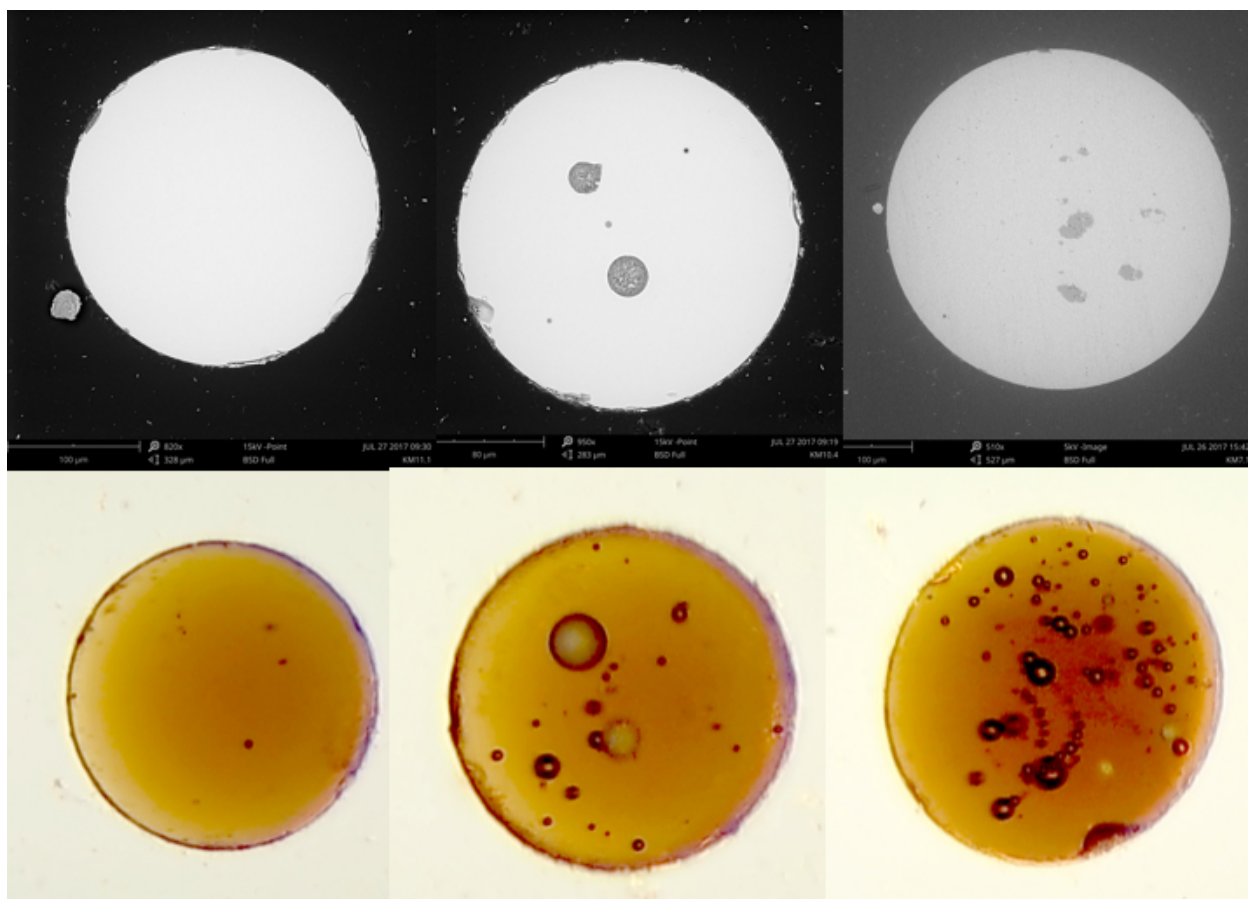


Figure 16. SEM (upper) and optical microscope images (lower) of the interior of a few Pele's spherules. The above SEM image correlates with lower optical microscope image below it. The images show the differences in the internal vesicle distribution. The images on the left show little to no vesicles, the middle images show some vesicles of varying sizes, and the right images show many vesicles with some directionality to them. The optical microscope is very helpful to analyze the interior of these spherules because it allows us to see through the translucent sphere.

In a previous study, Pele's tears (~5 mm long) from Kilauea have been exposed in epoxy to observe the interior and it was reported that the tears contain spherical vesicles that are evenly distributed throughout the body of the particles, but not at the margins, which have fewer, smaller vesicles (Porritt et al., 2012). The observations of the spherules in this study did not entirely agree with the previous results of Pele's tears. These spherules' interiors revealed non-uniform complexities. While all the vesicles were spherical, some spherules had large interior vesicles whereas others lacked vesicles entirely. There was

not a greater number density of vesicles in the center of the spherules than on the margins of the particles. The intact interior vesicles provided some evidence of fluid inclusions, and there may have been some crystalline formations inside the spheres' bubbles, but this was not confirmed.

7.4 Experimental Uncertainties

Uncertainties in the determination of dissolution rates come from various aspects of the experimental and computational aspects of the study, including some error in the solution concentration measurement and variations in the fluid flow rates. The errors on the sample concentrations do not exceed $\pm 10\%$. Fluid flow rate tended to decline over the week-long experiment presumably due to compaction of the ash in the column, which led to a varying flow rate over the experiment. It is likely, however, that a similar process may occur in nature as ash deposited compacts over time. Uncertainties in elemental concentrations were greater for more dilute samples, this was reported as a higher detection limit.

As it is very challenging to correctly recreate natural conditions in the laboratory, it is important to highlight the limitations of this experimental set-up. As highlighted in Witham et al. (2005), temperature, ratio of ash to water, flow rate, and ash density are all factors that vary in both leachate experiments and the natural environment. It is important to understand what is actually being tested. As these factors change so can the dissolution rates, therefore altering the results of this study.

8. Discussion

8.1 Trends in BET and Geometric Surface Areas

On the basis of the results of this study, it appears that volcanic ash morphology and chemical composition both affect dissolution rates of ions into the environment. Surface area of the volcanic ash over the leachate experiment was measured by BET analysis and calculated geometrically. These two methods provide the end-members of a range of surface areas that could be relevant to leaching rates in nature. While measured BET surface areas are likely an overestimate of natural conditions, calculated geometric surface areas are a gross underestimate of surface area. Thus, the surface areas of volcanic ash in natural environments are bracketed by the measured and calculated ranges of BET and geometric surface areas.

BET is a measurement of gas adsorption onto solid surfaces, normalized by sample mass. Kr gas is adsorbed within all the external and internal complexities of the ash particles. BET-measured surface areas are much larger due to the incorporation of external complexities of the ash, such as dust, and internal complexities, such as vesicles created by bubbles in the melt, which make the particles porous and permeable to krypton gas (but not necessarily to water). BET measured surface areas were two to three orders of magnitude larger than geometric surface areas. BET measured surface areas are considered a better estimate than geometric surface areas due to the incorporation of surface complexities which have a significant control on dissolution rates (Jeschke and Dreybrodt, 2002). Previous studies have nevertheless used geometric surface area to calculate rates (Wolff-Boenisch et al., 2004) (**Equation 3**); assuming a homogenous particle size distribution (equal counts of all sizes) and a spherical particle shape. In this

study, there is a wide range of particle sizes with a far greater number density in smaller sizes (**Figure 7**), and the ash particles are not spherical, except for the Kilauea spherules.

The first reason that BET surface area is much larger than geometric surface area is the incorporation of dust. Dust is the small end member of particle size, defined in this study as particles $< 5 \mu\text{m}$ in the longest dimension. Dust is different from volcanic ash in that ash is created by fragmentation of a magmatic foam, whereas dust is interpreted to be created by the natural milling of particles colliding in the eruptive column before deposition (Rose and Durant., 2009; Langmann, 2013). As particles collide, angular edges of the ash break off and settle on the surface of the particle. Due to its large surface area to volume ratio, dust plays a major role in BET measurements, but is not counted at all in geometric surface area calculations, as it is too difficult to correctly measure particles $< 5 \mu\text{m}$, and therefore are commonly ignored. With the use of pristine unhydrated ash, this study characterizes the contribution volcanic dust had on overall surface area per mass. Typically, in leaching studies, dust particles may be sieved away or can be artificially created by laboratory processes such as milling, completed to obtain a homogenous particle size distribution, or to understand the effects of natural milling in the environment (Genareau et al., 2016). Dust is extremely important to quantify because it significantly increases overall surface area per mass, and particles with dust (high surface area) can be leached more rapidly than surfaces with no dust.

The second reason that BET surface area is significantly greater than the geometric calculation is due to the particle's internal complexities, which provide surface area but not external size. The adsorption of Kr gas on and through the ash particle is not necessarily representative of how water reacts with the ash in nature. It is unlikely that

water moves through the ash particle the same way as krypton gas due to the large contrast in viscosities. However, water does come into contact with some unknown fraction of the ash particle's total surface and therefore can promote leaching from a portion of interior surfaces. If water gets stuck inside the particle, held by surface tension, the water would chemically behave as a batch experiment and reach saturation state rapidly. If this water is eventually able to escape this could release more ions, such as fluoride, into the water over longer time scales. This process is difficult to understand due to the micro-scale at which it occurs and should be a focus of future studies.

Using geometric and BET surface area trends, the surface area of the ash particles during the leaching experiment is interpreted to initially increase rapidly, decrease for some time, and then eventually increase. If the observed trend was extrapolated past the measured time it would be expected that the surface area would continue to increase due to the continued dissolution and shrinking of ash particles and therefore decreasing mass. The pattern of the change in BET surface area for basaltic and andesitic ashes is seemingly opposite from one another. Basaltic ash surface area decreased and then increased while the andesitic ash increased and then decreased. Upon closer investigation, it appears that these ashes likely follow the same pattern, but they do so over different time scales. The basaltic ash surface areas changed on a much shorter time-scale, so that the initial increase in surface area occurs before the first hour of leaching completes and begins to decrease after the first hour of the leaching. The initial increase is not shown in the BET record due to the coarse resolution of surface area data. This rapid change is likely because basaltic material weathers faster than andesitic material, and although these particles are glass, the chemical properties may cause them to behave

similar to crystal-bearing rock. The initial increase in surface area, seen in the BET data for andesitic ashes and the geometric surface area data, is interpreted to represent the initial disaggregation of the dust and small particles that are attached to larger particles. The bonds allowing ash particles to aggregate are potentially a combination of electrostatic forces and liquid bonds. Since some of the dust remains on the surface of the ash particles throughout the entire leaching experiment, the bonds adhering the dust to the particle are likely liquid bonds. The other evidence for liquid bonds over electrostatic bonds is that when the particles were analyzed under the SEM the electron beam did not destroy the bonds and cause the dust to move. After some time, depending on the sample, the initial dissolution of Na and Cl released some of the liquid salt-bonds that adhered dust to the surface of the ash particle (Brown et al., 2012; Mueller et al., 2016). As these bonds were partially dissolved by the water, some dust became loose. This loose dust increased overall surface area per mass, seen as the initial increase in surface area in the geometric surface areas for all samples and for the BET surface areas for andesitic samples (again it likely exists for the basaltic ashes, but is not seen in the surface area record). Overall surface area increased and mass remained constant, which allowed the overall surface area to mass ratio to increase. The liquid-bonds (NaCl) continued to dissolve over the week creating the balding effect that is seen in the SEM images of Turrialba ash (**Figure 9**). The smallest dust particles, which detached from the larger particles, are preferentially dissolved into the leachate. Small dust particles contribute a great deal of surface area per mass, but as soon as they dissolve completely, their contribution to surface area is eliminated, and thus surface area to mass ratio rapidly decreases. At that point, larger particles continue to shrink, thus increasing the overall

surface area to mass ratio. The BET method of analyzing surface area is critical to understand this process because this method accounts for the entire range of particle sizes.

The surface area trends are consistent between BET and geometric surface areas for the andesitic ashes but not for Eyjafjallajökull and Kilauea ashes. This is likely because the geometric surface area only takes into account particles $> 5 \mu\text{m}$ and only 150-200 particles were measured versus BET surface area which quantifies an entire gram of ash, potentially millions or more ash particles.

8.2 Metal Salts and Glass Dissolution

Results of this study showed how dissolution rates of major ions decayed rapidly, with some elements reaching a steady state dissolution rate after about an hour of the experiment. In part, the rapid decay in rate can be attributed to the soluble metal salts (which can be strong acids) on the particle's surface which dissolve into the water and dissociate to lower pH (Óskarsson, 1980; Smith et al., 1982; Frogner et al., 2001; Jones and Gislason, 2008). Evidence of acid formation can be seen in the initial drop in the pH record (**Figure 13**). It can also be seen in the two chemical populations clearly evident in the Kilauea record and somewhat in Turrialba (**Figure 12**). High initial surface areas of fresh leachable surfaces also contribute to the initial rapid decay of rates. Dust on the particle's surfaces initially provides a large amount of surface area to be leached. There is greater evidence that surface area has a stronger control on the rapid decay (and therefore dissolution rates), over soluble metal salts, as there is a large number density of small particles $> 20 \mu\text{m}$ contributing to surface area, versus in the chemical record which there

is only strong evidence for the dissolution for a second population of chemical interactions (metal salts versus glasses) for Kilauea. Once the surface dust is leached and there are no more readily available leachable surfaces, many ions reach steady state. During the initial period of rapid leaching (first hour), surface area increases due to disaggregation. However, disaggregation continues far longer than the initial rapid leaching event. **The decrease in leaching rate due to depletion of leachable ions from grain surfaces exceeds the addition of new surface area for leaching provided by disaggregation.**

Although some dissolution rates reach a background steady state rapidly, there are some small variations on the longer-term, week-long scale. Some of these variations can be attributed to flow rate. Flow rate slowed for all samples, sometimes from initial conditions of ~ 3 ml/ min to as low as ~ 0.05 ml/min. Throughout the experiment ash compressed in the columns making it more difficult for water to pass through. Similar issues with the flow rate have been reported in related studies (Jones and Gislason, 2008). Although this may have been a factor in long term rates it is not overall significant as concentrations range over a few orders of magnitudes whereas flow changes within an order of magnitude.

8.3 Environmental Implications

There is potential for short-term flora and fauna poisoning from volcanic leachates. Source water is most influenced by volcanic leaching, and is potentially unsafe for human or animal consumption, at the very beginning of the leaching when dissolution rate is highest. This would occur during the first rain event after deposition or during deposition into surface water. Ions detrimental to human health present in the ash-leachates include

F, Cu, Cd, Cr, As, and Se. While at most times throughout the leaching experiment the accumulated concentrations of ions (Cu, Cd, Cr, As, Se) fell below the World Health Organization (WHO) standards for safe drinking water, the ions remain in the environment and concentrations continue to accumulate from past and future eruptions. Therefore, there may be a significant health risks in active volcanic regions and water should be monitored for toxic levels from previous, current, and future eruptions.

Fluoride provides an excellent example of potential water contamination by ash leachates, particularly from basaltic Kilauea ash in this study. The WHO standard for fluoride in drinking water is 79 $\mu\text{mol/kg}$. This level was exceeded by leachate from all eruptions except Redoubt. There is significantly more F present in the pure basaltic Kilauea ash. High levels of F can potentially harm organisms with tissue including humans and animals, as chronic exposure to F leads to skeletal and dental fluorosis. This should be seriously considered in volcanic regions, especially in Hawaii and other areas subject to basaltic ash leaching. This also has implications for basalt rock weathering. A study completed in Northwestern Iran measured elevated concentrations of fluoride in groundwater coming from a basalt-alluvium aquifer (Moghaddam and Fijani, 2009). Although this study demonstrates that there is a linkage between basaltic weathering and high levels of fluoride, the main source of fluoride in groundwater is from minerals such as fluorite, fluorapatite, micas, amphiboles, topaz and rock phosphate and generally it has been found that basaltic rocks have a lower proportion of fluoride than granites (Hussain et al., 2004; Moghaddam and Fijani, 2009). We also see a high amount of F in the more silicic Turrialba ash. Independent of chemical composition of ash, fluoride has consistently proven to be a significant health concern in volcanic regions.

Although toxic waters can lead to poisoning of flora and fauna, the ash leachates also release nutrients such as N, P, K, Mg, Ca, and Fe that can lead to long-term fertilization in soils and short-term fertilization in the ocean. In the ocean, nutrients are rapidly consumed by phytoplankton since Fe is often a limiting nutrient in the ocean. Although it has been shown that an eruption can provide a concentrated release of Fe, the benefits will not last long after the supply of ash ceases. In soils, bioaccumulation of Mg, Ca and K allow the nutrients to remain in the area. This is seen in the formation of fertile volcanic soils which are used to grow important crops, such as coffee.

The environmental impacts reported in this study can be interpreted as an analog to natural conditions. The flow rate of 0.3 ml/min through the column used in this study, represents a percolation rate into the soils of 16 mm/hr. This rate represents a realistic percolation rate as rates near Turrialba volcano ranged from ~ 10-30 mm/hr (Toohey et al., 2018). Steady flow through a column best represents soil percolation or initial ash deposition into surface water. This is preferred over batch experiments, which would represent a static body of water that has no inflow or outflow.

9. Conclusions

Volcanic ash releases ions into surface water that can lead to both contamination and fertilization of natural and managed ecosystems. This can temporarily render surface water toxic to both humans and animals. The rate of leaching into the environment is controlled by both physical (surface area) and chemical (composition) characteristics of volcanic ash. When exposed to water, the volcanic ash has a rapid initial dissolution rate due to both a high number density of small particles and metal salts, which may decay to a background steady state dissolution rate in under an hour. Some of the dissolution rates

of ions from the glasses occur over a longer period, and some of them did not reach steady state in the week-long experiment. Surface area was measured by BET and calculated geometrically, and it was concluded that the change in surface area for basaltic ashes occurred on a shorter time scale than the andesitic ashes. It was also determined that the dissolution rates calculated with BET surface area were the more realistic estimate of natural conditions due to the inclusion of external and internal particle complexities. Chemically, although both the andesitic and basaltic ashes leach a wide range of ions, in this study it was found that basaltic ash from Hawaii leaches the highest concentration of fluoride, although the F from the dusty Turrialba ash was significant as well. These high levels of fluoride exceed the WHO standard for safe drinking water and pose a serious threat to both humans and livestock who may consume this water. The experimental results from the Column Leachate Tests can inform new and previous volcanic leachate models (Stewart et al., 2006), and provide a basis for assessing environmental impacts of a chemically broader range of volcanic eruptions around the world. Models can lead to better preparation for, and mitigation of, surface water contamination from current and future eruptions.

10. Future Research

Leachate studies, although expanding, still have a way to go before obtaining a complete understanding of chemical and physical interactions of volcanic ash with the environment. Volcanic dust is an important factor revealed in this study that is still not well understood. In this study, we suggest that dust is created by the milling of ash particles in the eruptive column, which then adheres onto the surface of the ash particles.

This has yet to be tested and confirmed. How is dust actually formed? We know that some of the dust and small particles dissolve into the leachate, but not all do. This could be due to the time frame on which the leachate experiment was completed. How much of the dust dissolves? Is there a way to trap and isolate dust so it can be tested in the laboratory? Is dust most prevalent on ash that comes from highly explosive eruptions within high ash columns? If this is the case then highly energetic eruptions are not only dangerous due to their explosiveness but because of their potential to produce highly dusty particles and therefore result in higher initial dissolution rates.

Another area of many unknowns is the mechanisms that allows ash to aggregate. How do ash aggregates bond, and how does it change throughout a leaching experiment? Is it a combination of both electrostatic forces and liquid bonds?

Another unknown in this field is how far into the particle's interior water penetrates under natural conditions and thus, how much is available to leaching. It would also be instructive to perform this study's methods on highly vesicular, rhyolitic ash. Fresh ash of this sort is very difficult to obtain due to the explosive and dangerous nature of eruptions that produce it. Hopefully in future studies some of these questions can be addressed to better understand the geochemical influence of a range of ash compositions and surface areas on the ecosystem and help provide an improved understanding of volcanic ash-ecosystem response.

11. References

- Achterberg, E. P., Moore, C. M., Henson, S. A., Steigenberger, S., Stohl, A., Eckhardt, S., ... Ryan-Keogh, T. J. (2013). Natural iron fertilization by the Eyjafjallajökull volcanic eruption. *Geophysical Research Letters*, 40(5), 921–926.
<https://doi.org/10.1002/grl.50221>
- Albersheim, S., & Guffanti, M. (2009). The United States national volcanic ash operations plan for aviation. *Natural Hazards*, 51(2), 275–285.
<https://doi.org/10.1007/s11069-008-9247-1>
- Araya, O., Wittwer, F., Villa, A., & Ducom, C. (1990). Bovine fluorosis following volcanic activity in the southern Andes. *Veterinary Record*, 126 (26), 641-642.
ISSN : 0042-4900
- Armienta, M. A., de la Cruz Reyna, S., Morton, O., Cruz, O., & Cenicerros, N. (2002). Chemical variation of tephra-fall deposit leachates for three eruptions from Popocatepelt volcano. *Journal of Volcanology and Geothermal Research*, 113, 61–80.
- Asghari Moghaddam, A., & Fijani, E. (2009). Hydrogeologic framework of the Maku area basalts, northwestern Iran. *Hydrogeology Journal*, 17(4), 949–959.
<https://doi.org/10.1007/s10040-008-0422-y>
- Attal, M., & Lavé, J. (2009). Pebble abrasion during fluvial transport: Experimental results and implications for the evolution of the sediment load along rivers. *Journal of Geophysical Research*, 114 (F4), 1-22.
<https://doi.org/10.1029/2009JF001328>
- Bagnato, E., Aiuppa, A., Andronico, D., Cristaldi, A., Liotta, M., Brusca, L., & Miraglia, L. (2011). Leachate analyses of volcanic ashes from Stromboli volcano: A proxy for the volcanic gas plume composition? *Journal of Geophysical Research Atmospheres*, 116(17), 1–17. <https://doi.org/10.1029/2010JD015512>
- Bau, M., Tepe, N., & Mohwinkel, D. (2013). Siderophore-promoted transfer of rare earth elements and iron from volcanic ash into glacial meltwater, river and ocean water. *Earth and Planetary Science Letters*, 364, 30–36.
<https://doi.org/10.1016/j.epsl.2013.01.002>
- Baxter, P. J., & Ancia, A. (2002). Human Health and Vulnerability in the Nyiragongo

- Volcano Crisis Democratic Republic of Congo, 2002. *Acta Vulcanologica*, 14(1–2), 109–114.
- Bosshard-Stadlin, S. A., Mattsson, H. B., Stewart, C., & Reusser, E. (2017). Leaching of lava and tephra from the Oldoinyo Lengai volcano (Tanzania): Remobilization of fluorine and other potentially toxic elements into surface waters of the Gregory Rift. *Journal of Volcanology and Geothermal Research*, 332, 14–25.
<https://doi.org/10.1016/j.jvolgeores.2017.01.009>
- Brantley S., White A. & Hodson M. (1999) Surface area of primary silicate minerals. In Growth, Dissolution and Pattern Formation in Geo-systems (eds. B. Jamtveit and P. Meakin). Chapman & Hall, London.
- Brown, R. J., Bonadonna, C., & Durant, A. J. (2012). A review of volcanic ash aggregation. *Physics and Chemistry of the Earth*, 45–46, 65–78.
<https://doi.org/10.1016/j.pce.2011.11.001>
- Browning, T. J., Stone, K., Bouman, H. A., Mather, T. A., Pyle, D. M., Moore, C. M., & Martinez-Vicente, V. (2015). Volcanic ash supply to the surface ocean: remote sensing of biological responses and their wider biogeochemical significance. *Frontiers in Marine Science*, 2(March), 1–22.
<https://doi.org/10.3389/fmars.2015.00014>
- Bull, K. F., Anderson, S. W., Diefenbach, A. K., Wessels, R. L., & Henton, S. M. (2013). Emplacement of the final lava dome of the 2009 eruption of Redoubt Volcano, Alaska. *Journal of Volcanology and Geothermal Research*, 259, 334–348.
<https://doi.org/10.1016/j.jvolgeores.2012.06.014>
- Bull, K. F., & Buurman, H. (2013). An overview of the 2009 eruption of Redoubt Volcano, Alaska. *Journal of Volcanology and Geothermal Research*, 259, 2–15.
<https://doi.org/10.1016/j.jvolgeores.2012.06.024>
- Cabré, J., Aulinas, M., Rejas, M., & Fernandez-Turiel, J. L. (2016). Volcanic ash leaching as a means of tracing the environmental impact of the 2011 Grímsvötn eruption, Iceland. *Environmental Science and Pollution Research*, 23(14), 14338–14353. <https://doi.org/10.1007/s11356-016-6559-7>
- Cangemi, M., Speziale, S., Madonia, P., D'Alessandro, W., Andronico, D., Bellomo, S., Brusca, L., Kyriakopoulos, K. (2017). Potentially harmful elements released by

- volcanic ashes: Examples from the Mediterranean area. *Journal of Volcanology and Geothermal Research*, 337, 16–28.
<https://doi.org/10.1016/j.jvolgeores.2017.03.015>
- Chichester, D. L., & Landsberger, S. (1996). Determination of the Leaching Dynamics of Metals from Municipal Solid Waste Incinerator Fly Ash Using a Column Test. *Journal of the Air and Waste Management Association*, 46(7), 643–649.
<https://doi.org/10.1080/10473289.1996.10467498>
- Cioni, R., Pistolesi, M., Bertagnini, A., Bonadonna, C., Hoskuldsson, A., & Scateni, B. (2014). Insights into the dynamics and evolution of the 2010 Eyjafjallajökull summit eruption (Iceland) provided by volcanic ash textures. *Earth and Planetary Science Letters*, 394(May 2010), 111–123.
<https://doi.org/10.1016/j.epsl.2014.02.051>
- Clague, D. A., Hagstrum, J. T., Beeson, M. H., & Champion, D. E. (1999). Kilauea summit overflows: Their ages and distribution in the Puna District, Hawai'i. *Bulletin of Volcanology*, 61(6), 363–381. <https://doi.org/10.1007/s004450050279>
- Coombs, M. L., Bleick, H. A., Cervelli, P. F., Bull, K. F., & Wessels, R. L. (2013). Volcano-ice interactions precursory to the 2009 eruption of Redoubt Volcano, Alaska. *Journal of Volcanology and Geothermal Research*, 259, 373–388.
<https://doi.org/10.1016/j.jvolgeores.2012.10.008>
- Cordeiro, S., Coutinho, R., & Cruz, J. V. (2012). Fluoride content in drinking water supply in São Miguel volcanic island (Azores, Portugal). *Science of the Total Environment*, 432, 23–36. <https://doi.org/10.1016/j.scitotenv.2012.05.070>
- Cronin, S. J., Hedley, M. J., Neall, V. E., & Smith, R. G. (1998). Agronomic impact of tephra fallout from the 1995 and 1996 Ruapehu Volcano eruptions, New Zealand. *Environmental Geology*, 34(1), 21–30. <https://doi.org/10.1007/s002540050253>
- Cronin, S. J., Neall, V. E., Lecointre, J. A., Hedley, M. J., & Loganathan, P. (2003). Environmental hazards of fluoride in volcanic ash: A case study from Ruapehu volcano, New Zealand. *Journal of Volcanology and Geothermal Research*, 121(3–4), 271–291. [https://doi.org/10.1016/S0377-0273\(02\)00465-1](https://doi.org/10.1016/S0377-0273(02)00465-1)
- Cronin, S. J., & Sharp, D. S. (2002). Environmental impacts on health from continuous volcanic activity at Yasur (Tanna) and Ambrym, Vanuatu. *International Journal*

- of Environmental Health Research*, 12(2), 109–123.
<https://doi.org/10.1080/09603120220129274>
- Cronin, S. J., Stewart, C., Zernack, A. V., Brenna, M., Procter, J. N., Pardo, N., ... Irwin, M. (2014). Volcanic ash leachate compositions and assessment of health and agricultural hazards from 2012 hydrothermal eruptions, Tongariro, New Zealand. *Journal of Volcanology and Geothermal Research*, 286, 233–247.
<https://doi.org/10.1016/j.jvolgeores.2014.07.002>
- Delmelle, P., Villi  ras, F., & Pelletier, M. (2005). Surface area, porosity and water adsorption properties of fine volcanic ash particles. *Bull Volcanol*, 67, 160–169
 DOI 10.1007/s00445-004-0370-x
- De Moor, J. M., Aiuppa, A., Avar  , G., Wehrmann, H., Dunbar, N., Muller, C., ... Galle, B. (2016). *Journal of Geophysical Research : Solid Earth*, 121, 5761-5775.
<https://doi.org/10.1002/2016JB013150>.Received
- Di Piazza, A., Rizzo, A. L., Barberi, F., Carapezza, M. L., De Astis, G., Romano, C., & Sortino, F. (2015). Geochemistry of the mantle source and magma feeding system beneath Turrialba volcano, Costa Rica. *Lithos*, 232, 319–335.
<https://doi.org/10.1016/j.lithos.2015.07.012>
- Durant, A. J., Villarosa, G., Rose, W. I., Delmelle, P., Prata, A. J., & Viramonte, J. G. (2012). Long-range volcanic ash transport and fallout during the 2008 eruption of Chait  n volcano, Chile. *Physics and Chemistry of the Earth*, 45–46, 50–64.
<https://doi.org/10.1016/j.pce.2011.09.004>
- Escudey, M., Arancibia-Miranda, N., Pizarro, C., & Antil  n, M. (2014). Effect of ash from forest fires on leaching in volcanic soils. *Catena*, 135, 383–392.
<https://doi.org/10.1016/j.catena.2014.08.006>
- Flaathen, T. K., & Gislason, S. R. (2007). The effect of volcanic eruptions on the chemistry of surface waters: The 1991 and 2000 eruptions of Mt. Hekla, Iceland. *Journal of Volcanology and Geothermal Research*, 164(4), 293–316.
<https://doi.org/10.1016/j.jvolgeores.2007.05.014>
- Frogner, P., Gislason, S. R., &   skarsson, N. (2001). Fertilizing potential of volcanic ash in ocean surface water. *Geology*, 29(6), 487–490. [https://doi.org/10.1130/0091-7613\(2001\)029<0487:FPOVAI>2.0.CO](https://doi.org/10.1130/0091-7613(2001)029<0487:FPOVAI>2.0.CO)

- Frogner Kockum, P. C., Herbert, R. B., & Gislason, S. R. (2006). A diverse ecosystem response to volcanic aerosols. *Chemical Geology*, 231(1–2), 57–66.
<https://doi.org/10.1016/j.chemgeo.2005.12.008>
- Fu, G., Lin, H. X., Heemink, A. W., Segers, A. J., Lu, S., & Palsson, T. (2015). Assimilating aircraft-based measurements to improve forecast accuracy of volcanic ash transport. *Atmospheric Environment*, 115, 170–184.
<https://doi.org/10.1016/j.atmosenv.2015.05.061>
- Gautier, J.-M., Oelkers, E., & Schott, J. (2001) Are quartz dissolution rates proportional to BET surface areas? *Geochim. Cosmochim. Acta*, 65, 1059–1070.
- Genareau, K., Cronin, S. J., Stewart, C., Bhattacharyya, S., & Donahoe, R. (2016). Post-eruptive impacts of pyroclastic deposits from basaltic andesite stratovolcanoes on surface water composition. *Journal of Geophysical Research: Biogeosciences*, 121(5), 1275–1287. <https://doi.org/10.1002/2015JG003316>
- Genareau, K., Mulukutla, G. K., Proussevitch, A. A., Durant, A. J., Rose, W. I., & Sahagian, D. L. (2013). The size range of bubbles that produce ash during explosive volcanic eruptions. *Journal of Applied Volcanology*, 2(1), 4.
<https://doi.org/10.1186/2191-5040-2-4>
- Genareau, K., Proussevitch, A., Durant, A., Mulukutla, G., & Sahagian, D. (2012). Sizing up the bubbles that produce very fine ash during explosive volcanic eruptions. *Journal of Geophysical Research*, 39(15), 1-6.
<https://doi.org/10.1029/2012GL052471>
- Genareau, K., Wardman, J. B., Wilson, T. M., McNutt, S. R., & Izbekov, P. (2015). Lightning-induced volcanic spherules. *Geology*, 43(4), 319–322.
<https://doi.org/10.1130/G36255.1>
- Gislason, S. R., Hassenkam, T., Nedel, S., Bovet, N., Eiríksdóttir, E. S., Alfredsson, H. A., ... Stipp, S. L. S. (2011). Characterization of Eyjafjallajökull volcanic ash particles and a protocol for rapid risk assessment. *Proceedings of the National Academy of Sciences*, 108(18), 7307–7312.
<https://doi.org/10.1073/pnas.1015053108>
- Gudmundsson, M. T., Thordarson, T., Hoskuldsson, A., Larsen, G., Björnsson, H., Prata, F. J., ... Jónsdóttir, I. (2012). Ash generation and distribution from the April-May

- 2010 eruption of Eyjafjallajökull, Iceland. *Scientific Reports*, 2, 1–12.
<https://doi.org/10.1038/srep00572>
- Horwell, C. J., Sparks, R. S. J., Brewer, T. S., Llewellyn, E. W., & Williamson, B. J. (2003). Characterization of respirable volcanic ash from the Soufrière Hills volcano, Montserrat, with implications for human health hazards. *Bulletin of Volcanology*, 65(5), 346–362. <https://doi.org/10.1007/s00445-002-0266-6>
- Hussain, J., Sharma, K.C., & Hussain, I., Fluoride in Drinking Water in Rajasthan and Its Ill Effects on Human Health. *Journal of Tissue Research*, 4(2), 263–273. ISSN: 0971 - 2283
- Jeschke, A. A., & Dreybrodt, W. (2002). Dissolution rates of minerals and their relation to surface morphology. *Science*, 66(17), 3055–3062.
- Jones, M. T., & Gislason, S. R. (2008). Rapid releases of metal salts and nutrients following the deposition of volcanic ash into aqueous environments. *Geochimica et Cosmochimica Acta*, 72(15), 3661–3680.
<https://doi.org/10.1016/j.gca.2008.05.030>
- Langmann, B. (2013). Volcanic Ash versus Mineral Dust: Atmospheric Processing and Environmental and Climate Impacts. *ISRN Atmospheric Sciences*, 2013(ii), 1–17.
<https://doi.org/10.1155/2013/245076>
- Madonia, P., Cangemi, M., Bellomo, S., & D'Alessandro, W. (2013). Influence of volcanic activity on the quality of water collected in roof water catchment systems at Stromboli Island (Italy). *Journal of Geochemical Exploration*, 131, 28–36.
<https://doi.org/10.1016/j.gexplo.2012.08.018>
- Millaleo, R., Reyes- Diaz, M., Ivanov, A. ., Mora, M. ., & Alberdi, M. (2010). Manganese As Essential and Toxic Element for Plants: Transport, Accumulation and Resistance Mechanisms. *Journal of Soil Science and Plant Nutrition*, 10(4), 470–481. <https://doi.org/10.4067/S0718-95162010000200008>
- Moen, W.S., & McLucas, G.B., (1980). Mount St. Helens ash: Properties and possible uses. Report of Investigation, vol. 24. Washington Department of Natural Resources, Division of Geology and Earth Resources. 60 pp.
- Mueller, S. B., Kueppers, U., Ayris, P. M., Jacob, M., & Dingwell, D. B. (2016). Experimental volcanic ash aggregation: Internal structuring of accretionary lapilli

- and the role of liquid bonding. *Earth and Planetary Science Letters*, 433, 232–240. <https://doi.org/10.1016/j.epsl.2015.11.007>
- Newhall, C.G., & Self, S., (1920). The volcanic explosivity index (VEI) an estimate of explosive magnitude for historical volcanism. *Journal of Geophysical Research*, 87 (C2) 1231-1238. <https://doi.org/10.1029/JC087iC02p01231>
- Olgun, N., Duggen, S., Croot, P. L., Delmelle, P., Dietze, H., Schacht, U., ... Garbe-Schönberg, D. (2011). Surface ocean iron fertilization: The role of airborne volcanic ash from subduction zone and hot spot volcanoes and related iron fluxes into the Pacific Ocean. *Global Biogeochemical Cycles*, 25(4), 1–15. <https://doi.org/10.1029/2009GB003761>
- Ono, K., Watanabe, K., Hoshizumi, H., Takada, H., & Ikebe, S. (1995). Ash eruption of Nakadake Crater, Aso Volcano, Southwestern Japan, *Journal of Volcanology and Geothermal Research*, 66, 137–148.
- Óskarsson, N. (1980). The interaction between volcanic gases and tephra: Fluorine adhering to tephra of the 1970 hekla eruption. *Journal of Volcanology and Geothermal Research*, 8(2–4), 251-266. [https://doi.org/10.1016/0377-0273\(80\)90107-9](https://doi.org/10.1016/0377-0273(80)90107-9)
- Óskarsson, N. (1981). The chemistry of icelandic lava incrustations and the latest stages of degassing. *Journal of Volcanology and Geothermal Research*, 10(1–3), 93–111. [https://doi.org/10.1016/0377-0273\(81\)90057-3](https://doi.org/10.1016/0377-0273(81)90057-3)
- Parfitt, E. A. (1998). A study of clast size distribution, ash deposition and fragmentation in a Hawaiian-style volcanic eruption. *Journal of Volcanology and Geothermal Research*, 84(3–4), 197–208. [https://doi.org/10.1016/S0377-0273\(98\)00042-0](https://doi.org/10.1016/S0377-0273(98)00042-0)
- Porritt, L. A., Russell, J. K., & Quane, S. L. (2012). Pele’s tears and spheres: Examples from Kilauea Iki. *Earth and Planetary Science Letters*, 333–334, 171–180. <https://doi.org/10.1016/j.epsl.2012.03.031>
- Rose, W. I., & Durant, A. J. (2009). Fine ash content of explosive eruptions. *Journal of Volcanology and Geothermal Research*, 186(1–2), 32–39. <https://doi.org/10.1016/j.jvolgeores.2009.01.010>
- Rose, & Durant. (2011). A new perspective on continental moisture recycling. *Eos Trans. AGU*, 90(52), Fall Meet. Suppl., Abstract H41G-0988-Oral.

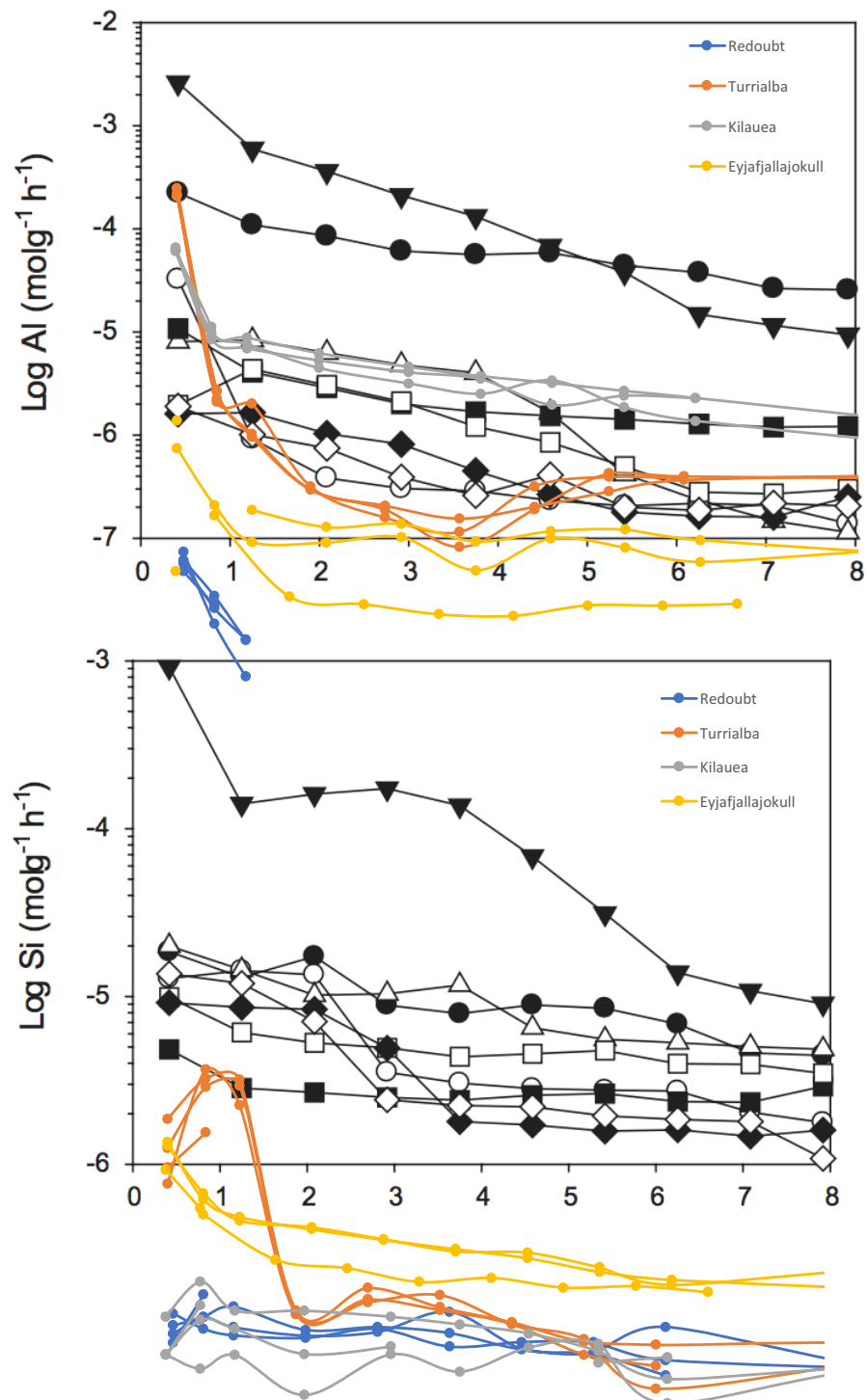
<https://doi.org/10.5194/acp>

- Rubin, C. H., Noji, E. K., Seligman, P. J., Holtz, J. L., Grande, J., & Vittani, F. (1994). Evaluating a fluorosis hazard after a volcanic eruption. *Archives of Environmental Health*, 49(5), 395–401. <https://doi.org/10.1080/00039896.1994.9954992>
- Scott, W.E., & McGimsey, R.G., (1994). Character, mass, distribution, and origin of tephra-fall deposits of the 1989–1990 eruption of Redoubt volcano, south–central Alaska. *Journal of Volcanology and Geothermal Research*, 62, 251–272.
- Smith, D.B., Zielinski, R.A., & Rose, W.I., (1982). Leachability of Uranium and Other Elements From Freshly Erupted Volcanic Ash. *Journal of Volcanology and Geothermal Research*, 13, 1-30.
- Stewart, C., Johnston, D. M., Leonard, G. S., Horwell, C. J., Thordarson, T., & Cronin, S. J. (2006). Contamination of water supplies by volcanic ashfall: A literature review and simple impact modelling. *Journal of Volcanology and Geothermal Research*, 158(3–4), 296–306. <https://doi.org/10.1016/j.jvolgeores.2006.07.002>
- Swanson, D. A. (2008). Hawaiian oral tradition describes 400 years of volcanic activity at Kīlauea. *Journal of Volcanology and Geothermal Research*, 176(3), 427–431. <https://doi.org/10.1016/j.jvolgeores.2008.01.033>
- Taylor, A. S., Blum, J. D., & Lasaga, A. C. (2000a). The dependence of labradorite dissolution and Sr isotope release rates on solution saturation state. *Geochimica et Cosmochimica Acta*, 64(14), 2389–2400. [https://doi.org/10.1016/S0016-7037\(00\)00361-6](https://doi.org/10.1016/S0016-7037(00)00361-6)
- Taylor, A. S., Blum, J. D., Lasaga, A. C., & MacInnis, I. N. (2000b). Kinetics of dissolution and Sr release during biotite and phlogopite weathering. *Geochimica et Cosmochimica Acta*, 64(7), 1191–1208. [https://doi.org/10.1016/S0016-7037\(99\)00369-5](https://doi.org/10.1016/S0016-7037(99)00369-5)
- Taylor, H.E., & Lichte, F.E. (1980). Chemical Composition of Mount St. Helens Volcanic Ash. *Geophysical Research Letters*, 7(11), 949–952.
- Tester, J.W., Worley, W.G., Robinson, B.A., Grigsby, C.O., & Feerer, J.L. (1994). Correlating quartz dissolution kinetics in pure water from 25 to 625°C. *Geochimica et Cosmochimica Acta*, 58 (11) 2407-2420. [https://doi.org/10.1016/0016-7037\(94\)90020-5](https://doi.org/10.1016/0016-7037(94)90020-5)

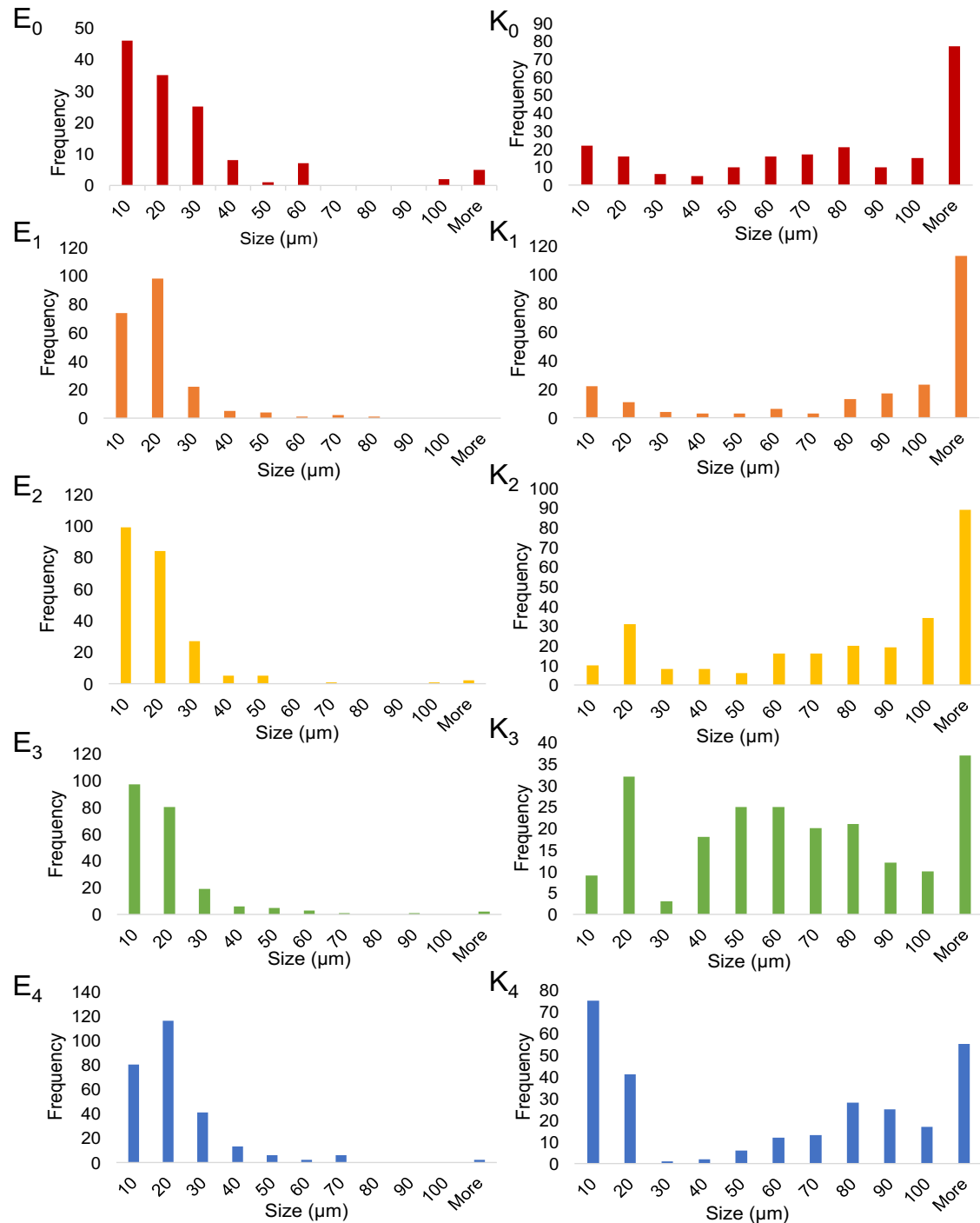
- Thordarson, T. (2003). Atmospheric and environmental effects of the 1783–1784 Laki eruption: A review and reassessment. *Journal of Geophysical Research*, 108(D1), 4011. <https://doi.org/10.1029/2001JD002042>
- Toohey, R.C., Boll, J., Brooks, E.S., & Jones, J.R. (2018). Effects of land use on soil properties and hydrological processes at the point, plot, and catchment scale in volcanic soils near Turrialba, Costa Rica. *Geoderma*, 315, 138–148. <https://doi.org/10.1016/j.geoderma.2017.11.044>
- Toramaru, A. (2014). On the second nucleation of bubbles in magmas under sudden decompression. *Earth and Planetary Science Letters*, 404, 190–199. <https://doi.org/10.1016/j.epsl.2014.07.035>
- Van Manen, S., Avar, G., & Martínez-Cruz, M. (2015). Co-ideation of disaster preparedness strategies through a participatory design approach: Challenges and opportunities experienced at Turrialba volcano, Costa Rica. *Design Studies*, 40, 218–245. <https://doi.org/10.1016/j.destud.2015.06.002>
- van Manen, S. M. (2014). Hazard and risk perception at Turrialba volcano (Costa Rica); implications for disaster risk management. *Applied Geography*, 50, 63–73. <https://doi.org/10.1016/j.apgeog.2014.02.004>
- Walker, G. P. L. (1981). Generation and dispersal of fine ash and dust by volcanic eruptions. *Journal of Volcanology and Geothermal Research*, 11(1), 81–92. [https://doi.org/10.1016/0377-0273\(81\)90077-9](https://doi.org/10.1016/0377-0273(81)90077-9)
- Wilson, T., Stewart, C., Cole, J., Johnston, D., & Cronin, S. (2010). Vulnerability of farm water supply systems to volcanic ash fall. *Environmental Earth Sciences*, 61(4), 675–688. <https://doi.org/10.1007/s12665-009-0380-2>
- Witham, C. S., Oppenheimer, C., & Horwell, C. J. (2005). Volcanic ash-leachates: A review and recommendations for sampling methods. *Journal of Volcanology and Geothermal Research*, 141(3–4), 299–326. <https://doi.org/10.1016/j.jvolgeores.2004.11.010>
- Wolff-Boenisch, D., Gislason, S. R., Oelkers, E. H., & Putnis, C. V. (2004). The dissolution rates of natural glasses as a function of their composition at pH 4 and 10.6, and temperatures from 25 to 74°C. *Geochimica et Cosmochimica Acta*, 68(23), 4843–4858. <https://doi.org/10.1016/j.gca.2004.05.027>

12. Appendices

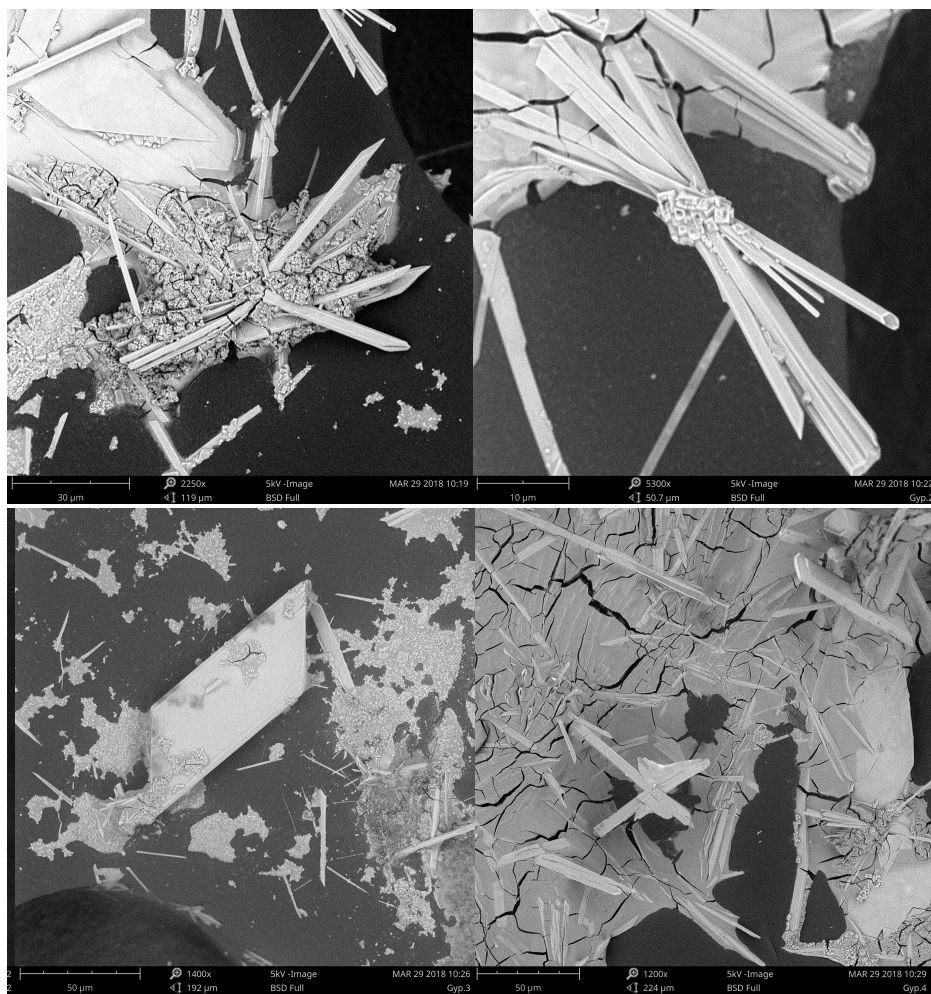
Appendix A. Fluxes of Al and Si from the Jones and Gislason (2008) leaching experiment of volcanic ash in de-ionized water. Flux results from this study are overlaid on the figure.



Appendix B. Measured particle size distribution, using the SEM and Image J, of Eyjafjallajökull (left column) and Kilauea (right column) ash over one week. Frequency of particles is plotted on the Y-axis and binned sizes of the particles in μm is on the X-axis. Subscripts equal the time that the ashes were leached for. 0: Initial ash before leachate test, 1: Post 1 hour of leaching, 2: Post 8 hours of leaching, 3: Post 4 days of leaching, 4: Post 7 days of leaching. Greatest number density of particles is $< 20 \mu\text{m}$ for both populations.



Appendix C. SEM images of the gypsum Turrialba precipitated weeks after the leaching experiment. Gypsum chemistry was confirmed using EDS.



Appendix D. Chemical concentrations from ICP-MS and IC. BET and geometric surface area data. Mass, pH, and flow rate data. Calculated flux data and dissolution rates calculated with both BET and geometric surface areas: Attached as supplemental data files

Appendix E. Column leachate test data from Redoubt, Turrialba, Eyjafjallajökull, and Kilauea: Attached as supplemental data files

13. Vita

Candace Wygel was born and raised in Clifton Park, NY. She graduated magna cum laude with honors from Skidmore College in Saratoga Springs, NY in 2016 with a BA in Geosciences and English. During her undergraduate career, she worked as a research assistant in a stable isotope lab at Skidmore and completed an REU internship at the American Museum of Natural History. After completing her MS in Earth and Environmental Science at Lehigh University this May, she plans to move to NYC and start a career in environmental consulting. She is also an avid creative science-fiction writer and plans to publish her novel in the future.